CHARACTERIZING A REGION OF BOVINE CHROMOSOME 6 ASSOCIATED WITH THREE CATTLE COAT COLOR PHENOTYPES

A Thesis

by

KATHY SCIENSKI

Submitted to the Office of Graduate and Professional Studies of
Texas A&M University
in partial fulfillment of the requirements for the degree of

MASTER OF SCIENCE

Chair of Committee,	Clare A. Gill
Committee Members,	Penny Riggs
	David Riley
	David Stelly
Interdisciplinary Faculty Chair,	Dorothy Shippen

August 2018

Major Subject: Genetics

ABSTRACT

Coat color of mammals, especially mice, has been a valuable model for the study of adaptation, pleiotropy, and gene action and interactions. More recently, however, the characterization of coat color in livestock has begun to identify genes associated with and causing different coat color phenotypes. Color is an especially important attribute in livestock as it is often a required component of breed recognition and registration. There are also numerous point-of-sale marketing programs designed to offer economic premiums for certain colors. Pigmentation in purebred cattle typically follows a pattern of Mendelian inheritance, but crossbred cattle often produce colors that are atypical of purebred cows. The aim of this study was to characterize a region on bovine chromosome 6 previously associated with three cattle coat color phenotypes in a population of Nellore-Angus crossbred cattle: gray, reddening, and white spotting. Genome-wide association studies (GWAS) were performed for the gray and spotting phenotypes using high-density SNP genotypes, and the regions associated with all three phenotypes were fine mapped. GWAS identified the same genes associated with gray and spotting phenotypes found in previous studies—*CORIN* and *KIT*, respectively. Fine mapping revealed that the $E^{+}E^{+}$ genotype at *MC1R* coupled with a mutation within *CORIN* was coincident with the gray phenotype, although later findings suggest that these factors are necessary but not sufficient for gray. A missense variant in *CHIC2* was identified in the whole-genome sequenced founders contributing to $E^{D}E^{+}$ red animals. Additionally, founder data indicated that *KIT* and the region associated with white spotting lies within a poorly assembled region of the bovine genome. Haplotype breed of origin also tends to influence all three phenotypes. Histological examinations of skin and hair revealed that gray coat color in this population results when white

hair occurs atop dark-pigmented skin, and that lack of hair pigmentation is due to both melanocyte depletion and displacement.

ACKNOWLEDGEMENTS

I would like to thank my committee chair, Dr. Clare Gill, and my committee members, Dr. Penny Riggs, Dr. David Riley, and Dr. David Stelly, for their guidance, support, and patience throughout the course of this research.

I am incredibly grateful to my lab members, Bailey Engle, Guosong Wang, and Yue (July) Xing, for their guidance and camaraderie. Thank you, Guosong, for having the solution to any bioinformatics problem I encountered and always sharing a laugh. Thank you, July, for sharing your wisdom of CNVs. And a special thank you, Bailey, for your daily dose of inspiration, "Bailey-capes," and a friendship I wouldn't dare to trade.

I owe a great deal of thanks to Dr. Jim Mazurkiewicz for reminding me of the important things in life, introducing me to countless new opportunities and connections, and always having the utmost faith in me—dziękuję serdecznie!

Additionally, I wish to thank Michael Kamradt for teaching me how to perform immunohistochemistry, the kind staff at the VIBS Histology Laboratory for their aid and expertise, and Dr. Alessandro Bagnato at the University of Milan for hosting me in Italy during my last semester.

Thanks also to my parents, Marek and Irena, and in-laws, Rob and Deb, for constantly pushing me and always being just a phone call away.

Finally, and most importantly, I want to thank my wonderful husband, Seth Hirst. I absolutely could not have come this far without his unwavering encouragement, patience, and love. Thank you for always being my light.

CONTRIBUTORS AND FUNDING SOURCES

This work was supervised by a thesis committee consisting of Dr. Clare Gill, advisor, Dr. Penny Riggs and Dr. David Riley of the Department of Animal Sciences and Dr. David Stelly of the Department of Soil and Crop Sciences.

Phenotype scores for all animals were provided by Dr. Clare Gill, Dr. David Riley, and Dr. Jim Sanders. Imputation was performed by Dr. Clare Gill. Whole genome sequence data and SNP genotypes were provided by Dr. Clare Gill.

The histology for Sections 3.1 and 3.2 was performed by the VIBS Histology Laboratory. In Section 3.2, paraffin sections were provided by the VIBS Histology Laboratory, while immunohistochemistry was conducted in part by Michael Kamradt. All other work conducted for the thesis was completed by the student independently.

Graduate study was supported by a fellowship from the National Institute of Food and Agriculture within the U.S. Department of Agriculture, National Needs Fellowship (2014-38420-21835).

NOMENCLATURE

BP	Base Pair
BTA	Bovine Chromosome
CNV	Copy Number Variant
GWAS	Genome-Wide Association Study
H&E	Haematoxylin & Eosin
IHC	Immunohistochemistry
KB	Kilobase
MB	Megabase
SNP	Single Nucleotide Polymorphism

TABLE OF CONTENTS

Page

LIST OF FIGURES

Page

LIST OF TABLES

Page

1. INTRODUCTION AND LITERATURE REVIEW

1.1 Objective

In order to characterize the functional candidates associated with gray, red, and white spotted phenotypes in Nellore-Angus crossbred cattle, the objective of this project is to refine the critical interval on bovine chromosome 6 previously associated with all three phenotypes.

1.2 Importance of coat color

Coat colors of livestock and laboratory animals have been studied for decades. Documentation of coat color dates back as far as the Paleolithic period, evidenced by cave paintings in present-day France portraying large animals with a seemingly vast variety of colors and patterns. These variations in coat color have played a prominent role in discussions of environmental adaptation and mechanisms driving evolution for years (Enshell-Seijffers *et al.* 2008).

Biological ramifications of color range from camouflage and mate selection, to UV protection and parasite defense (Roulin *et al.* 2001; da Silva *et al.* 2003; Fang *et al.* 2009; Hubbard *et al.* 2010). In livestock, color is often utilized as a breed registration requirement and breed recognition tool. In fact, color serves such great economic importance in U.S. beef production that DNA tests for coat color are already in place by the industry, as premiums or discounts can be provided for certain colors. Color has also played a historic role in selection. The inspection criteria for Hanwoo cattle in the 1930's, for example, promoted the exclusion of animals with black or striped hair. And later, Hanwoo cattle with white spots were eliminated in the effort to unify the breed's appearance (Choi *et al.* 2012).

The attribute also serves as an avenue to examine gene action and interaction, as many coat color phenotypes reflect a close relationship between genotype and phenotype and demonstrate Mendelian inheritance. Genes known to be involved in melanogenesis—the process by which pigment is produced—have also surfaced in genome-wide association studies and other reports unrelated to coat color, implying pleiotropic effects and functionality across an array of tissues and phenotypes, both in livestock (Hecht 2006; Philipp *et al.* 2011; Jacobs *et al.* 2016) and other mammals (Hager *et al.* 1998; Harris *et al.* 2001; Kuklin *et al.* 2004; Hecht 2006; Perez-Guisado *et al.* 2006; Wu 2007; Rapley *et al.* 2009; Siddiq *et al.* 2012; Reissmann & Ludwig 2013; Cantanhede & de Oliveira 2017).

1.3 Melanogenesis

Melanogenesis is by definition the process underlying the production of pigment, or melanin. In mammals, melanin is the main determinant of skin, hair, and eye color, but it is also found in the substantia nigra area of the brain in the form of neuromelanin (Zecca *et al.* 2001). During embryogenesis, melanocytes, the pigment-producing cells, are derived from pluripotent neural crest cells that then become melanoblasts. These melanoblasts migrate from the truncal neural crest, then along the dorsolateral pathway, and finally non-randomly enter developing hair follicles in the skin, populating the basal layer of the epidermis (Tobin & Paus 2001; Slominski *et al.* 2005; Steingrimsson *et al.* 2005). Melanogenesis can occur at the cellular level (follicular melanocytes), organ level (hair follicle), and during development (Slominski *et al.* 2005). The process is subject to influences such as hormones, pH level within the skin, age, and ethnicity (Slominski *et al.* 2005; Simon *et al.* 2009; D'Mello *et al.* 2016).

Within melanocytes, melanin is synthesized in specialized organelles termed melanosomes. These are a type of lysosome-related organelle that also originate from endosomes and multivesicular bodies. Proteins necessary for melanosome formation or melanin synthesis are transported to the melanosome as it matures. As a result, different stages of melanosomes (I-IV) contain varying proteins and amounts of melanin (Amsen 2009). After melanin is produced, the melanosomes make their way to the dendritic ends of the melanocyte by means of microtubules and actin filaments, and keratinocytes then phagocytose the melanosomes whole (Ohbayashi *et al.* 2012; Wu *et al.* 2012).

In the skin, one melanocyte is surrounded by approximately 36 keratinocytes, while in the hair bulb, there is one melanocyte for every five keratinocytes (Tobin & Paus 2001; Riley & Borovansky 2011). In contrast to continuous melanogenesis in the skin, hair pigmentation is active only during the anagen stage (growth phase) of the hair cycle. Melanogenesis is switched off in the catagen stage (end of anagen or the transitional phase that allows the follicle to renew itself) and subsequently remains absent through telogen (dormant stage) (Slominski & Paus 1993). Because of this, melanocytes in hair follicles are more sensitive to aging influences than those in the skin (Tobin & Paus 2001).

The two types of melanin that can be produced are eumelanin (brown/black) and pheomelanin (yellow/red). Although synonyms may have been used in the literature, throughout this section, the genes and corresponding proteins contributing to melanogenesis will be identified by the official names for human genes and proteins from the HGNC (Gray *et al.* 2015) and Uniprot (The UniProt Consortium 2017) databases, respectively. Abbreviations for proteins are capitalized, whereas genes are both capitalized and italicized. Factors affecting which melanin will be produced include tyrosinase related protein 1 (TYRP1), dopachrome tautomerase

(DCT), high free-cysteine concentrations, and/or tyrosinase (TYR) activity (Hida *et al.* 2009). Tyrosine serves as the starting material for the biosynthesis of melanin, but then eumelanogenesis and pheomelanogenesis diverge after oxidation by TYR of tyrosine to dopaquinone, also known as the Mason-Raper pathway, or the rate-limiting step of melanogenesis (Pawelek & Korner 1982; Oetting 2000). After this step, the synthesis of pheomelanin requires the addition of cysteine to dopaquinone, forming 5-S-cysteinyl-DOPA or 2-S-cysteinyl-DOPA. Alternatively, dopaquinone can enter the eumelanin-specific pathway by oxidation to dopachrome, which is further processed to form the two building blocks of eumelanin: 5,6-dihydroxyindole (DHI) and 6-dihydroxyindole-2-carbolic acid (DHICA). Tyrosinase related protein 1 and DCT are needed in addition to TYR for the formation of eumelanin (Ito & Wakamatsu 2008), as DCT is what promotes the production of DHICA in tautomerization of dopachrome (Simon *et al.* 2009).

A variety of other genes and gene products play a role in melanogenesis. Premelanosome protein (PMEL) and the protein melanoma antigen recognized by T-cells 1 (MART-1) produced by the gene melan-A (*MLANA*), for example, are critical structural proteins (Yamaguchi *et al.* 2007), whereas biogenesis of lysosome-related organelles complex 1 (BLOC-1) and P protein (produced by OCA2 melanosomal transmembrane protein, *OCA2*) play important roles in sorting and trafficking melanosomes (Sitaram & Marks 2012). Paired box 3 (*PAX3*) contributes to cell survival and growth in the melanocytic lineage and is known to help regulate the transition from early melanoblasts derived from the neural crest to mature melanocytes (Scholl *et al.* 2001; He *et al.* 2005). Additionally, KIT proto-oncogene receptor tyrosine kinase (*KIT*) and KIT ligand (*KITLG*) are essential for melanocyte development.

Melanogenesis comprises of multiple pathways, including the Protein Kinase C (PKC), cyclic AMP (cAMP), MAPK/ERK Kinase (MEK), and Wingless-related integration site (WNT) pathways. But, before these pathways can commence, a series of events must occur on the surface of the cell. Melanocyte stimulating hormone receptor (MSH-R), produced by the gene melanocortin receptor 1 (*MC1R*), a positive regulator of hair pigmentation, must become bound by either alpha melanocyte-stimulating hormone (α-MSH), a POMC cleavage product, or ASP (produced by agouti signaling protein, or *ASIP*) in order for the intracellular signal transduction cascade to commence. Genetic, biochemical, and pharmacological evidence have established that signaling from MSH-R is the main factor dictating melanogenesis (Riley & Borovansky 2011). This protein is a seven transmembrane G-protein coupled receptor and has an intracellular C-terminus with a palmitoylation site and an extracellular N-terminus with an N-linked glycosylation site (Wolf Horrell *et al.* 2016). Binding to this protein is mutually exclusive by α-MSH and ASP (Wolf Horrell *et al.* 2016). Pheomelanin synthesis is promoted with ASP binding (Videira *et al.* 2013). Proopiomelanocortin (*POMC*) gene products for MSH-R are expressed in the skin in a hair-cycle dependent manner, with low levels at telogen and high levels during anagen development (Slominski & Paus 1993). Unlike pheomelanogenesis, eumelanogenesis is ultimately stimulated via the melanocyte-stimulating hormone receptor (MSH-R) agonist alpha melanocyte-stimulating hormone (α-MSH) (Videira *et al.* 2013; D'Mello *et al.* 2016). After α-MSH exposure, MSH-R becomes desensitized in a protein kinase A (PKA)-independent and G-protein coupled receptor kinase-dependent manner. β-arrestins then bind the phosphorylated receptor and prevent it from coupling to the G-protein, as well as target the receptor for internalization (Wolf Horrell *et al.* 2016). ASP-MSH-R signaling, on the other hand, is cAMP-independent and uses attractin (ATRN) and E3 ubiquitin-protein ligase mahogunin ring finger 1

(MGRN1) (Hida *et al.* 2009). Another peptide proposed to alter melanocortin signaling is β-defensin. Although its role in modulation has not been fully characterized, it is thought to act in one of three ways: (1) bind to and activate MSH-R, (2) bind to MSH-R and prevent its inhibition by ASP, or (3) bind to ASP, leading to its sequestration and/or degradation (Candille *et al.* 2007; Walker & Gunn 2010a; Wolf Horrell *et al.* 2016).

Figure 1, reprinted with permission from the Kyoto Encyclopedia of Genes and Genomes (KEGG) (Kanehisa & Goto 2000; Kanehisa *et al.* 2016; Kanehisa *et al.* 2017), illustrates the four pathways through which melanin can be produced—Protein Kinase C (PKC), cyclic AMP (cAMP), MEK, or WNT. Members of the protein kinase C pathway are encoded by nine genes and are classified into three subclasses based on their requirements for activation. Microphthalmia-associated transcription factor (produced by melanogenesis associated transcription factor, *MITF*) serves as a transcription factor for PKCβ, which is then activated by diacylglycerol. This in turn induces its translocation from the cytoplasm to the membrane where it phosphorylates and activates tyrosinase, thus inducing melanogenesis (D'Mello *et al.* 2016). The cAMP pathway possesses a much different scheme and can be activated when either mast/stem cell growth factor receptor Kit (SCFR, produced by the gene *KIT*) or MSH-R become bound. This pathway upregulates melanin synthesis through PKA activation, cAMP response element binding protein (CREB) phosphorylation, *MITF* expression and increased transcription of *TYR* and related genes (Amsen 2009). When PKA becomes activated, it upregulates transcription factor SOX-9 (produced by SRY-box 9, or *SOX9*) and CREB, both of which regulate the *MITF* promoter. Transcription factor SOX-9 and microphthalmia-associated transcription factor then act together to regulate the *DCT* promoter, while microphthalmia-associated transcription factor additionally acts on the *TYR* promoter to upregulate

melanogenesis (D'Mello *et al.* 2016). The most important role of transcription factor SOX-9, however, may lie in its ability to induce the expression of SRY-box 10 (*SOX10*) in melanoblast development (Aoki *et al.* 2003; Cheung & Briscoe 2003). Transcription factor SOX-10 dictates the transcription of *MITF*, which in turn controls a set of genes critical for melanogenesis including *DCT*, *PMEL*, and *TYRP1*. In fact, in the absence of transcription factor SOX-10, *MITF* cannot induce the expression of *TYR* (Hou *et al.* 2006).

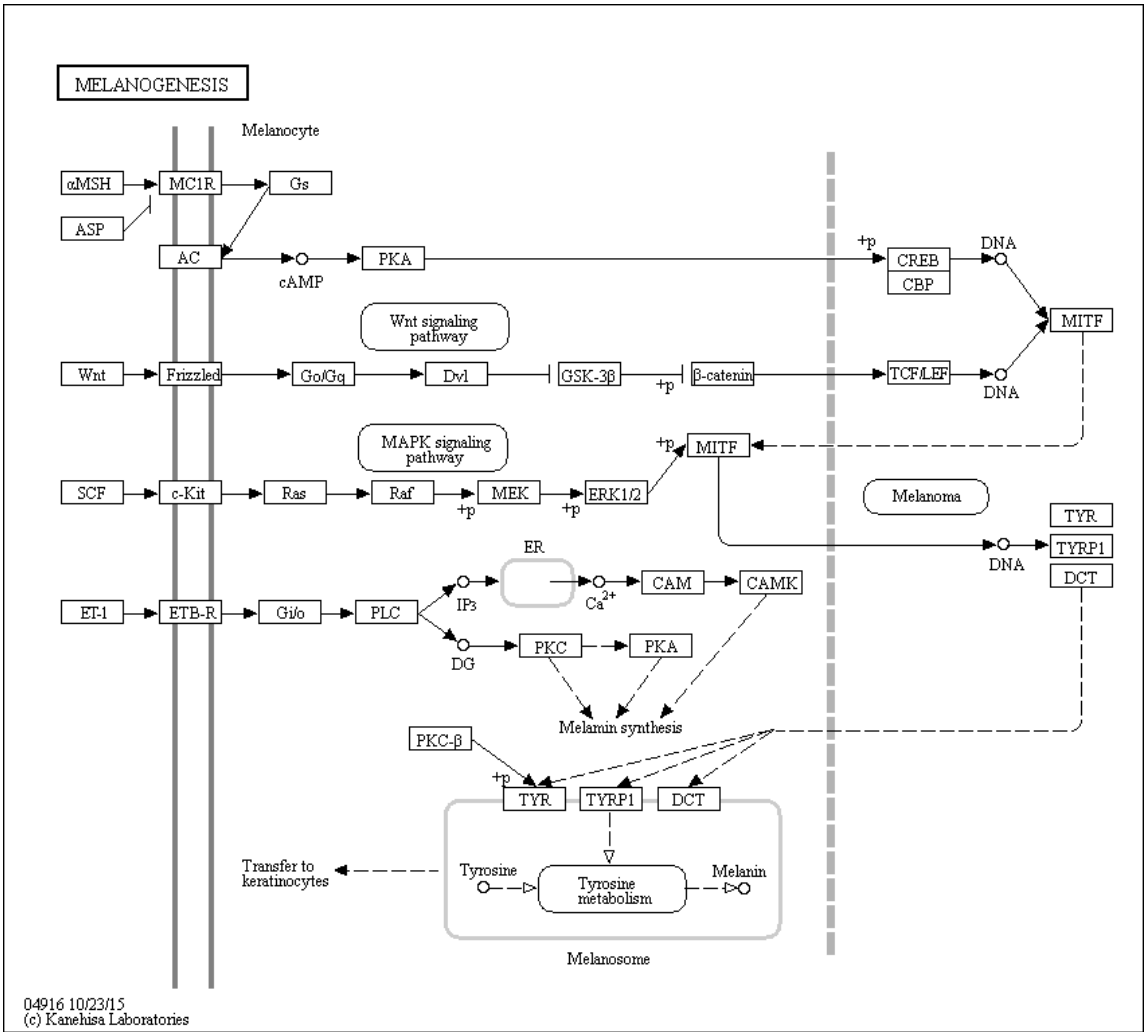

Figure 1. KEGG melanogenesis reference pathway (map04916). Reprinted with permission from KEGG: Kyoto Encyclopedia of Genes and Genomes. Copyright 2018 by Kanehisa Laboratories.

The MEK pathway is straightforward, as Ras (a small GTPase) becomes activated when MSH-R becomes bound. It then activates a series of mitogen-activated protein kinases (MAP3K, MAP2K, and MAPK), which eventually leads to the phosphorylation of *MITF* (D'Mello et al. 2016). The WNT pathway is fairly simple as well, as it directly acts on *MITF*. Wnt proteins bind to their receptors which in turn increases the stability of cytoplasmic β-catenin, leading to transport of β-catenin into the nucleus and thus regulating transcription of *MITF* through interactions with TCF/LEF transcription factors (Steingrimsson *et al.* 2004). Moreover, Wnt signaling plays a critical role in melanogenesis as a whole. Proto-oncogene Wnt-1 (produced from Wnt family member 1, *WNT1*) signals to melanoblasts to increase the number of melanocytes, while protein Wnt-3a (from Wnt family member 3A, *WNT3A*) acts on melanoblasts to maintain *MITF* expression and promotes melanoblast differentiation into melanocytes. Protein Wnt-3a also partners with β-catenin to promote the differentiation of neural crest cells into melanocytes (Jin *et al.* 2001; Dunn *et al.* 2005). β-catenins are essential, not only because of their role in *MITF* transcription regulation in this pathway, but also due to their influence on other genes involved in melanogenesis. β-catenin activity has been known to suppress *ASIP* expression and activate serine protease corin (*CORIN)*, for example (Enshell-Seijffers *et al.* 2010).

Each of these melanin-producing pathways affects or is affected by *MITF*; whether it's phosphorylating *MITF* (MEK), regulating the transcription of *MITF* (cAMP, WNT), or having *MITF* as its transcription factor (PKC). The regulation of multiple pigmentation and differentiation related-genes by *MITF* has strengthened the hypothesis that *MITF* functions as a central regulator of melanogenesis (D'Mello *et al.* 2016). This master regulator has been known to alter the expression of *TYR*, *TYRP1*, and *DCT* by directly binding to cis-elements within their

promoter sequences (Shin *et al.* 2016). Within *MITF* itself, the M promoter is targeted by several transcription factors including paired box protein Pax-3, CREB, transcription factor SOX-9, transcription factor SOX-10, LEF-1, and ONECUT-2, as some have been previously mentioned (Levy *et al.* 2006; D'Mello *et al.* 2016).

1.4 Coat color in cattle

Klungland *et al.* (1995) identified MSH-R, the *MC1R* protein product, as a primary driver of base coat color phenotypes in cattle. *MC1R* was named as the extension locus, and its alleles follow a dominance series of $E^D > E^+ > e$. The presence of a dominant E^D allele causes black coat color, whereas the E^+ allele produces a receptor that responds to both α-MSH and ASP, leading to a full range of color from yellow to black. The *e* allele produces a red coat color when present in the homozygous state because the receptor is inactive due to truncation of the MSH-R protein (Klungland *et al.* 1995). Angus can have either black or red coat color, whereas Nellore have black skin covered by a white or light gray coat. Crossbred cattle often have an array of phenotypes that arise from mechanisms outside of *MC1R* function, or rather produce colors that are atypical of purebred cows (Allison 2009; Rolf 2015). Gray, red, and spotted coat colors have all been observed in both crossbred and purebred cattle.

Histological examination of hair in other mammals, namely mice, has determined that gray coloration is often due to the loss of melanocytes, but the cause of this phenotype in cattle has not yet been determined (Silvers 1979). Breeds that are gray by nature include Tyrolean Grey, Murray Gray, Gascon, and Nellore. Some producers find the gray phenotypes favorable and are incorporating these breeds into their cattle composites as a way to avoid black coat color (Phillips 2017). Nevertheless, gray coat color has also been observed in crossbred cattle. A

recent report identified a region on BTA 6 associated with gray coat color in Nellore-Angus crossbred cattle (Holland 2015), while other reports have described gray color in Charolais composites (Olson 1999; Gutierrez-Gil *et al.* 2007; Kuhn & Weikard 2007; Rolf 2015). The gray color observed in Charolais crosses has been attributed to a dilution phenomenon involving *PMEL*, a gene producing a critical structural protein for melanin. Dilution of the hair itself has been found to be caused by one of three phenomena: (1) reduction in tyrosinase activity of hair bulbar melanocytes, (2) defective migration of melanocytes from a reservoir in the upper outer root sheath to dermal papilla, or (3) suboptimal melanocyte-keratinocyte interaction (Tobin & Paus 2001).

Reddening of the cattle coat is most commonly due to the *e*/*e* genotype at *MC1R*, as previously stated. However, there have been reports of red coat color mediated through other genetic avenues, both in purebred and crossbred cattle. Variant and dominant red phenotypes have both been identified in the Holstein breed, and red in Highland cattle has also been characterized. A gene interaction with *DEFB103* allows Holstein cattle with an E^D/- genotype to display the variant red phenotype indistinguishable from cattle with an *e*/*e* genotype at *MC1R* (Dreger & Schmutz 2010). On the other hand, Holstein cattle with a missense mutation within coatomer protein complex, subunit alpha (*COPA*) display the dominant red phenotype. This is also similar to the recessive red phenotype, although comparatively less effective at reducing eumelanin synthesis (Dorshorst *et al.* 2015). Highland cattle possessing E^+/*e* or *e*/*e* *MC1R* genotypes are red, but only if they do not harbor a deletion at *PMEL* (Schmutz & Dreger 2013).

Red coat color in crossbreds has been identified in both Nellore-Angus and Charolais-Holstein stock. A report addressing the degree of reddening in Nellore-Angus crossbred cattle found multilocus influences on the phenotype, with a locus on bovine chromosome (BTA) 6

overcoming the dominant E^D allele at *MC1R*. The Nellore allele must be in a homozygous state at the BTA 6 locus in order for this phenomenon to occur (Hanna *et al.* 2014). Conversely, the same Charolais x Holstein crossbred population that reported gray coat color also reported a red color that arose from the same dilution event. *PMEL*, coupled with a locus on BTA 28 and including lysosomal trafficking regulator (*LYST*), were proposed modifiers of the *Dc* locus (Gutierrez-Gil *et al.* 2007).

White spotting is characteristic of several dairy breeds and has also been observed in Hereford, Simmental, Fleckvieh, and various crossbreds. In all of these instances, *KIT* or *MITF* is responsible for the unpigmented hair (Table 1). Mutations within *KIT* have permitted spotting in Holstein, Hereford, Hereford crosses, and Holstein-Friesian x Jersey crossbred cattle (Grosz & MacNeil 1999; Reinsch *et al.* 1999; Liu *et al.* 2009; Fontanesi *et al.* 2010b). *MITF*, on the other hand, is responsible for white spotting and dominant white. This gene was first found to cause dominant white in German Fleckvieh cattle (Philipp *et al.* 2011) and is also shown to be correlated with spotting in Italian Holstein and Italian Simmental breeds (Fontanesi *et al.* 2012).

Table 1. Genes involved in cattle coat color.

Gene	Phenotype	Reference(s)
ASIP	Brindle	(Girardot *et al.* 2006)
COPA	Dominant red	(Dorshorst *et al.* 2015)
CORIN	Yellow	(Shin *et al.* 2016)
	Gray	(Holland 2015)
DEFB103	Variant red	(Dreger & Schmutz 2010)
IGFBP7	Proportion of black	(Fan *et al.* 2014)
KIT	White spotting	(Grosz & MacNeil 1999; Fontanesi *et al.* 2010b)
	Degree of white	(Reinsch *et al.* 1999; Liu *et al.* 2009; Brenig *et al.* 2013; Fan *et al.* 2014)
	Color sidedness	(Durkin *et al.* 2012)
KITLG	Roan	(Charlier *et al.* 1996; Seitz *et al.* 1999)
MC1R, E^D	Dominant black	(Klungland *et al.* 1995; Han *et al.* 2011)
MC1R, e/e	Red	(Klungland *et al.* 1995)
MITF	Degree of white spotting	(Liu *et al.* 2009; Fontanesi *et al.* 2012)
	Dominant white	(Philipp *et al.* 2011)
MLPH	Dilution	(Li *et al.* 2016; Dikmen *et al.* 2017)
TWIST2	White belt	(Drogemuller *et al.* 2009; Awasthi Mishra *et al.* 2017)
TYR	Albinism	(Schmutz *et al.* 2004)
TYRP1	Dun brown/dilution	(Nonneman *et al.* 1996; Berryere *et al.* 2003)
PDGFRA	Reddening	(Hanna *et al.* 2014)
	Proportion of black	(Fan *et al.* 2014)
PMEL/SILV	Dilution	(Hecht 2006; Gutierrez-Gil *et al.* 2007; Kuhn & Weikard 2007; Schmutz & Dreger 2013)

1.5 Gray, red and spotted phenotypes in other mammals

Gray

Lifelong gray coat color, as opposed to progressive graying, is often documented as a dilution of eumelanin, due in part to inadequate melanin presence, or as a result of pigment-type switching of individual hairs that the human eye perceives as a single color. Dilution of black

pigment creates a gray shade often termed “blue,” and can be observed in the rabbit, dog, cat, and mouse; melanophilin (*MLPH*) is responsible for this dilution in these four mammals (Silvers 1979; Philipp *et al.* 2005; Ishida *et al.* 2006; Lehner *et al.* 2013; Fontanesi *et al.* 2014). Meanwhile, pigment-type switching of individual hairs can give the appearance of an all-over gray coat. Gray mice, for example, may have a mixture of white-tipped, all-white, or black and white individual hairs for the “silver-gray” phenotype. A mutation within *PMEL* is the cause for this phenomenon (Silvers 1979). Gray wolves, on the other hand, require mutations at both *CBD103* and *ASIP* to produce individual hairs containing eumelanin and pheomelanin alike (Anderson *et al.* 2009).

Conversely, gray can also be produced as a standalone color unrelated to dilution or pigment-type switching events. This is evident in the mink, pig, and horse. Mink demonstrate an Aleutian, or gun-metal gray, phenotype that is caused by deletion of a single nucleotide in exon 40 of lysosomal trafficking regulator (*LYST*), whereas pigs can be gray-roan because of a 4 bp deletion within a single copy of *KIT* (Fontanesi *et al.* 2010a; Anistoroaei *et al.* 2013). Mutations in horses have been observed within *PMEL* (missense mutation in exon 11) and syntaxin 17 (*STX17*) (4.6 kb duplication in intron 6) for the silver and gray phenotypes, respectively (Brunberg *et al.* 2006; Rosengren Pielberg *et al.* 2008; Kavar *et al.* 2012).

Red

Red coat color in cattle is generally attributed to a recessive genotype (*e*/*e*) at *MC1R*. This *e* allele is caused by a frameshift mutation, resulting in a truncated MSH-R and the production exclusively of pheomelanin. A similar phenomenon exists in other mammals, such as the dog, horse, cat, donkey, and rabbit, where a mutation in *MC1R* is responsible for red coloration

(Marklund *et al.* 1996; Fontanesi *et al.* 2006; Schmutz & Berryere 2007; Peterschmitt *et al.* 2009; Abitbol *et al.* 2014; Gustafson *et al.* 2017). Cats and dogs can also exhibit red coat color two other ways: a premature stop codon within *TYRP1* for a reddish-brown hue (cats), or a combination of alleles at *ASIP* for a fawn appearance (dogs) (Schmidt-Kuntzel *et al.* 2005; Schmutz & Berryere 2007).

White spotted

The *KIT* gene is the most common contributor to white spotting in mammals, though a handful of other genes have also been identified as influential to the phenotype. A series of mutations in *MITF*, for example, cause white spotting in the dog, horse, and buffalo (Schmutz *et al.* 2009; Hauswirth *et al.* 2012; Baranowska Korberg *et al.* 2014; Yusnizar *et al.* 2015; Negro *et al.* 2017). Horses have also demonstrated other avenues for spotting with mutations in endothelin receptor B (*EDNRB*), *PAX3*, and transient receptor potential cation channel subfamily M member 1 (*TRPM1*), resulting in areas of unpigmented hair (Santschi *et al.* 1998; Hauswirth *et al.* 2012; Bellone *et al.* 2013; Hauswirth *et al.* 2013). Other livestock animals, such as the sheep and goat, display a dominant white phenotype by means of a CNV within *ASIP* (Fontanesi *et al.* 2009; Han *et al.* 2015). In spite of this, *KIT* is most often responsible for white spotting in mammals due to its role in driving melanocyte migration during development. Supporting evidence for white spotting attributable to *KIT* can be observed in the horse, fox, camel, donkey, cat, and dog, among other mammals (Brooks & Bailey 2005; Brooks *et al.* 2007; Haase *et al.* 2009; Gerding *et al.* 2013; Hauswirth *et al.* 2013; Wong *et al.* 2013; David *et al.* 2014; Yan *et al.* 2014; Haase *et al.* 2015; Capomaccio *et al.* 2017; Durig *et al.* 2017; Holl *et al.* 2017a; Holl *et al.* 2017b; Negro *et al.* 2017).

1.6 Present status of the problem and corresponding candidate genes

Gray

Holland (2015) categorically scored Nellore-Angus crossbred cattle as gray (similar to "cases" in disease studies, n = 33) or not gray (similar to "controls" in disease studies, n = 723) (Holland 2015). Scoring was conducted at weaning and again at adulthood to verify that animals were gray over the duration of their lifetime, as opposed to exhibiting progressive graying. Red-tinged cattle consistently possessing gray hair were also classified as being gray and were subsequently incorporated into the statistical analyses in order to account for any misclassifications or discrepancies in the scoring procedure (Fig. 2). Three evaluators later validated the phenotypic scores using photographs of each animal. Two genome-wide associations using 34,957 single nucleotide polymorphisms (SNP) genotypes were conducted, either excluding or including red-tinged gray individuals (n = 42). Results identified *CORIN* on bovine chromosome (BTA) 6 as the strongest candidate gene associated with gray in this cross (Holland 2015).

CORIN encodes a mosaic protein (atrial natriuretic peptide-converting enzyme) and is vital for pro-atrial natriuretic peptide (pro-ANP) activation in the heart (Wu 2007). Although *CORIN* has been primarily studied for its function in the heart, there have been reports of this gene playing a role in coat color. A recent study characterized *CORIN* expression in the hair follicle and deemed it to be a negative regulator of *ASIP*. Mice in this study that were homozygous for a *CORIN* mutation had overall lighter coats due to an increased amount of pheomelanin in the hair shaft (Enshell-Seijffers et al. 2008). Moreover, *CORIN* has been proposed to play a role in the yellow coat color of Hanwoo cattle (Shin *et al.* 2016).

Figure 2. Nellore-Angus cattle scored for gray. (a-f) Individuals classified as gray. (g-h) Individuals classified as red-tinged gray.

Red

An observation was made that some cattle from the Texas A&M McGregor Genomics Cycle 1 Population possessing a single copy of the E^D allele at *MC1R* were not black, contrary to the dominance model of $E^D > E^+ > e$, and instead were red. Consequently, the cattle in this cycle were quantitatively scored for degree of black (Hanna *et al.* 2014). The study identified a region on BTA 6 that interacts with *MC1R* to control degree of reddening in Nellore-Angus cattle; the Nellore allele was deemed recessive in this region on BTA 6. Candidates for this phenomenon included *CORIN*, *PDGFRA*, and *KIT*. A follow-up study subsequently refined the reddening region on BTA 6, extracted RNA from ear notches on individuals within the study, and subjected genes both in the reddening region and those known to have roles in melanogenesis to qRT-PCR (Womack 2015). No significant differences in expression were observed in the candidate genes previously suggested, but a new positional candidate of *CHIC2* was proposed.

CHIC2, a member of a highly conserved family of proteins characterized by a cysteine-rich hydrophobic domain, has not been previously documented for having a role in pigmentation. *CHIC2* is most well-known for its role in the *FIP1L1-PDGFRA* fusion seen in eosinophilia patients, in which the gene becomes uniformly deleted (Pardanani *et al.* 2003). However, its protein was identified to be localized to the plasma membrane and vesicular structures, and its cysteine-rich hydrophobic domain largely resembles cysteine-string proteins which are also known to bind to vesicular structures by means of palmitoylation (Cools *et al.* 2001).

White spotted

Animals from the same population and cycle as used in the prior reddening study were assigned scores for spotting based on the presence of areas of white hair on either or both the body and face (Fig. 3). Two genome-wide association studies (unpublished work) using 34,957 SNP genotypes were conducted using the categorical variables of white spots (n = 96) versus no white spots. The first study included all spotted animals, while the second included only those with facial spots (n = 33). Genome-wide significant SNP on BTA 6 within the previously identified region associated with gray and reddening phenotypes were identified. Based on previous spotting studies in livestock and other mammals, as well as its known role in melanogenesis and development, *KIT* was hypothesized as the functional candidate for the spotting phenotype.

Figure 3. Nellore-Angus cattle scored for white spotting. (a-d) Individuals scored only for facial spotting. (e-h) Individuals scored for body spots; some also have facial spots.

2. MATERIALS AND METHODS

2.1 Ethics statement

All procedures involving animals were reviewed and approved by the Texas A&M University Institutional Animal Care and Use Committee (AUP 2015–011A).

2.2 Cattle population

Cattle were raised at the Texas A&M AgriLife Research Center in McGregor, Texas. Nellore-Angus F_2 cattle were produced in the herd's first cycle (Cycle 1) via embryo transfer and were part of 13 full-sibling Nellore-Angus families; sire breed is listed first. These families were produced from 4 F_1 Nellore-Angus sires and 13 Nellore-Angus dams. A second F_2 group (Cycle 2) produced by natural service consisted of all 4 reciprocal crosses: Nellore-Angus x Nellore Angus, Nellore-Angus x Angus-Nellore, Angus-Nellore x Nellore-Angus, and Angus-Nellore x Angus-Nellore. Bulls and cows from the original embryo transfer Cycle 1 group were mated to produce F_3 calves (Cycle 3). Cycle 4 calves made up the F_4 generation; calves were produced by natural service matings of F_3 bulls to F_3 cows (Holland 2015). Cattle for Cycle 1 were produced in spring and fall calving seasons, whereas only a spring calving season was used for subsequent cycles.

2.3 Phenotypes and genotypes

Phenotypes

Scores assigned for each phenotype (gray, red, and white spotted) were previously assigned and largely based on animal photographs from Cycle 1. Briefly, calves were

photographed at birth, steers were photographed in the feeding pens, and females were photographed shortly after each calving. Some photographs were taken in the spring/summer whereas others were taken in the fall/winter. In all instances, photographs were scored separately and independently.

Gray was scored categorically (gray or not gray) by three evaluators as previously described by Holland (2015). Two of the evaluators assessed animals from Cycles 1 to 4 in person, and all three evaluated photographs of Cycle 1. The gray phenotype was measured or scored over the course of an animal's lifetime to ensure that the individual displayed a lifelong gray color rather than progressive graying with age. Several red-tinged gray individuals were identified and were incorporated with the gray individuals to account for any bias between evaluators.

Hanna *et al.* (2014) determined reddening (or degree of black) scores solely using photographs of each animal from Cycle 1. The phenotype was classified from 1 (lightly black; mostly red) to 9 (solid black) from photographs by three evaluators and a consensus score was determined. Dates of images and season of photographs (summer being May to October and winter being November to April due to seasonal changes in Texas) were constructed as a two-level fixed effect to reduce bias in scoring (Hanna *et al.* 2014).

Spotting was scored categorically (white spot(s) or no white spot(s)) for two phenotypes based on photographs of cattle from Cycle 1. The first phenotype features individuals with facial spotting, whereas the other contains those with body spots. Some individuals overlap within these categories, as they display spots in both locations. Females with white spots on their udder were incorporated into the body spots.

SNP Genotypes

As part of a larger project, blood samples were previously collected at weaning on calves in the F_2 generation and beyond for isolation of DNA as described by Riley *et al.* (2013). Briefly, for Cycle 1 cattle, 200 mL of blood was collected, whereas 30 mL was collected from subsequent cycles. High quality DNA was extracted from white blood cells or semen by standard proteinase K digestion and organic extraction methods. Genotypes were obtained using the Infinium BovineSNP50 assay (Illumina, Inc., San Diego, CA); version 1 chip was used on Cycle 1, while version 2 chip was used on Cycle 2 and Cycle 3 samples. Version 1 and 2 data were merged using PLINK software (Purcell *et al.* 2007). Usable data for 34,957 SNPs per animal was generated, with 26,692 informative markers per F_2 family (Riley *et al.* 2013; Holland 2015). The F_0 and F_1 generations were later genotyped with a high density (770,000) SNP chip (Illumina, Inc., San Diego, CA).

Additionally, all calves from Cycle 1 were genotyped for *MC1R* (RefSeq NM_174108.2) using the E3 and E4 primers designed by Klungland et al. (Klungland *et al.* 1995), which amplifies a 739 bp fragment of *MC1R* encompassing the SNP c.296C>T (E^+ to E^D allele) and the deletion c.311delG (*e* allele) (Hanna *et al.* 2014).

Whole Genome Sequencing and Imputation

There were 7 Nellore bulls and 6 Angus cows, which were founders of the Cycle 1 population that contributed to at least 10 calves in the F_2 generation of the cross. Fast Track DNA Sequencing Services (Illumina, Inc., San Diego, CA) prepared libraries for 100 bp paired-end sequencing. Each of the founder animals was sequenced to a depth of at least 30x genome coverage (i.e. ~80 Gb DNA sequence). As described by Gill (2016) raw reads were obtained

from Illumina in standard fastq format (Cock *et al.* 2010). After QC with fastq-mcf (Aronesty 2011), reads were aligned to the UMD3.1 bovine assembly (Zimin *et al.* 2009) with BWA (Li & Durbin 2009), and local realignment and recalibration of quality scores was done using GATK 3.2 (McKenna *et al.* 2010). SNP and indels were called using HaplotypeCaller (DePristo *et al.* 2011; Van der Auwera *et al.* 2013). SNP quality was recalibrated using VariantRecalibrator by applying BovineHD SNP that passed QC and bovine SNP from dbSNP138 as truth sets.

SNP genotypes were imputed up to the density of usable markers from the HD chip (553,344 markers) at the genome-wide level, and to sequence-scale (1,177,091 SNP) at the chromosome-wide level (BTA 6) using FImpute software (Sargolzaei *et al.* 2014) as described in (Gill 2016). Due to the multigenerational nature of the cattle population, imputation accuracy was high at 98.45%.

2.4 Statistical software

Several software packages were utilized to visualize and analyze data. PLINK was used in the management of data (Purcell *et al.* 2007), and GEMMA was used for genome-wide association studies (GWAS) by implementing the Genome-wide Efficient Mixed Model Association algorithm for linear mixed models. GEMMA implemented marker association tests with one phenotype and accounted for population stratification and sample structure, as well as estimated the proportion of variance explained (PVE) by fitting a univariate linear mixed model (Zhou & Stephens 2012). Upon receiving GWAS results from GEMMA, Integrative Genomics Viewer (IGV) and R software were used for data visualization and generating Manhattan plots. The purpose of this visualization was to identify SNP associated with each phenotype at the chromosome- and genome-wide levels. Analyses used Bonferroni correction at α=0.05 (genome:

$\alpha/n_{tests}=9.04 \times 10^{-8}$, chromosome: $\alpha/n_{tests}=4.25 \times 10^{-8}$). IGV was also used to examine the whole-genome sequence data of the population founders, as the tool has the ability to visualize mutations (i.e. translocations and deletions) (Robinson *et al.* 2011). Moreover, SAMtools was used to extract the raw reads and sequence data for the whole-genome sequenced founders (Li *et al.* 2009).

FastPhase was used to extract genomic regions and subsequently phase and construct haplotypes in order to track breed of origin through the pedigree and identify candidate positions concordant with each phenotype (Scheet & Stephens 2006).

2.5 Histology and immunohistochemistry

Histology

Histology was performed on a subset of individuals in the gray and reddening studies; the reddening study utilized 6mm skin biopsies collected from the flank with a punch biopsy and both studies used half inch-wide ear notches obtained from a clean 'V' cut ear notcher; skin samples were collected in the spring. All samples were immediately immersed in paraformaldehyde fix solution for 24 hours; skin was removed from each side of the ear notches before immersion. Samples were dehydrated using an ethanol series, and then embedded in paraffin in an orientation for longitudinal cross sectioning. Sections were microtomed at 5 μm thickness using a microtome designed by Leica Biosystems and mounted onto ColorFrost™ Plus Microscope Slides (Thermo Fisher Scientific, Waltham, MA).

H&E staining was performed only for those individuals in the gray study. Slides were deparaffinized and rehydrated by immersion in xylene three times for three minutes each, then in 100% ethanol for the same time period. Sections were then placed in 95% ethanol for three

minutes, in 80% ethanol for three minutes, and finally in deionized water for five minutes. Hematoxylin staining was performed by submerging sections in hematoxylin for three minutes, then rinsing them with deionized water and subsequently with tap water for five minutes. Slides were then dipped 10 times in acid ethanol, rinsed twice for one minute each time in tap water, then rinsed again for two minutes in deionized water. Successively, eosin staining and dehydration were executed by placing slides in eosin for 30 seconds, then thrice in 95% ethanol for five minutes each time, and again in 100% ethanol for three times at five minutes each. Lastly, sections were placed in xylene three times for 15 minutes each time, and Permount™ was added as a mounting medium prior to applying a coverslip to the slides.

Melanin bleach staining was carried out for samples in both the gray and reddening studies. Slides were made in triplicate for each animal, then deparaffinized and rehydrated in the same procedure as described above. The first set of slides were immersed in potassium permanganate for one hour, then 1% oxalic acid (OA) was added. The second set of slides were immersed in potassium permanganate for two hours, then 1% OA was added. Finally, the third set of slides were immersed in potassium permanganate for one hour, but no oxalic acid was added to the slides afterwards. These three methods were executed in order to identify which method most effectively provided the best staining results. All three sets of slides were then washed in tap water, H&E stained, and then dehydrated, cleared, and coverslipped, as described above.

Immunohistochemistry

Immunohistochemistry was only executed for samples in the reddening study. The paraffin wax on the sections was melted for one hour at 60ºC. Slides were immersed in xylene

three times for 15 minutes each round, then again in 100% ethanol for the same time periods. Slides were then transferred to 95% ethanol for five minutes, then to 70% ethanol for five minutes, and finally to distilled water for five minutes. Deparaffinized slides were immersed in a Coplin jar filled with 0.01 M sodium citrate pH 6.0 solution. The Coplin jar was placed inside a pressure cooker, which was then set on high pressure for 15 minutes. The Coplin jar was then placed on the lab bench for 30 minutes, and deionized water was gently run over the slides in the jar to cool the solution to room temperature, being careful not to detach the tissue from the slides. An ImmEdge™ Hydrophobic Barrier Pap Pen (H-4000) was used to circle the tissue on each slide, then slides were rinsed with 5 mL 0.05% phosphate buffered saline with Tween-20 (PBS-T). PBS-T pH 7.4 was created by combining 8mM Na_2HPO_4, 150mM NaCl, 2mM KH_2PO_4, 3mM KCl, and 0.05% Tween® 20. Tissue samples were incubated in 5% fetal bovine serum diluted in 0.05% PBS-T for one hour at room temperature. The polyclonal primary antibody of CHIC2 (Thermo Fisher Scientific, Waltham, MA) was diluted in 0.05% PBS-T and incubated overnight at 4ºC. Slides were then rinsed thrice with 0.05% PBS-T for five minutes, then three more times in 0.05% PBS-T for 10 seconds. A biotinylated anti-rabbit IgG secondary antibody (Thermo Fisher Scientific, Waltham, MA) was diluted 1:200 and incubated at room temperature for 30 minutes. Slides were rinsed with 0.05% PBS-T for five minutes (x3), then again with 0.05% PBS-T for 10 seconds (x3). Next, 100 microliters of Avidin-Biotin Complex (ABC) reagent (Thermo Fisher Scientific, Waltham, MA) was added to each slide at room temperature for 30 minutes. Slides were rinsed again with 0.05% PBS-T for five minutes (x3), and again with 0.05% PBS-T for 10 seconds (x3). Diaminobenzidine (DAB) reagent (Abcam) was prepared according to kit instructions. Slides were rinsed once with PBS (without Triton X) for 10 seconds. Tissue sections were then incubated in DAB reagent in dark for five minutes, and

the DAB reagent was aspirated from tissue sections. Slides were gently rinsed under tap water for five minutes, quickly dipped three times in 50% Richard-Allan Scientific™ Gill™ III Hematoxylin (Thermo Fisher Scientific, Waltham, MA), and then gently rinsed under running cold tap water for five minutes. Slides were then placed in 70% ethanol for five minutes, 95% ethanol for five minutes, 100% ethanol for five minutes (three times), and finally transferred to xylene for five minutes (three times). Lastly, slides were mounted with Permount™.

Microscopy and photography of the histology and IHC slides were conducted with the Eclipse Ni-E Upright Microscope from Nikon Instruments, Inc.

3. RESULTS AND DISCUSSION

3.1 Gray

A genome-wide association study using 553,344 SNP genotypes for 560 animals was conducted for gray (n=33) vs. not gray (n=527) with *MC1R* genotypes fitted as a fixed effect. A relationship matrix was also integrated into the model. The most significant SNP was located, as expected, within *CORIN* at 68059441 ($P_{raw}=1.50 \times 10^{-10}$, $P_{adjusted}=8.30 \times 10^{-5}$) on BTA 6 (Fig. 4). These genotypes were imputed to high density (1,177,091 SNP) on BTA 6 for 1,107 animals. A chromosome-wide association analysis was conducted for gray (n=53) vs. not gray (n=1,054) in this group, again incorporating *MC1R* genotypes as a fixed effect and a genomic relationship matrix. The lead SNP appeared again within *CORIN* at 68038658 bp ($P_{raw}=5.10 \times 10^{-7}$, $P_{adjusted}=0.60$), but did not survive multiple testing correction at $P<0.05$.

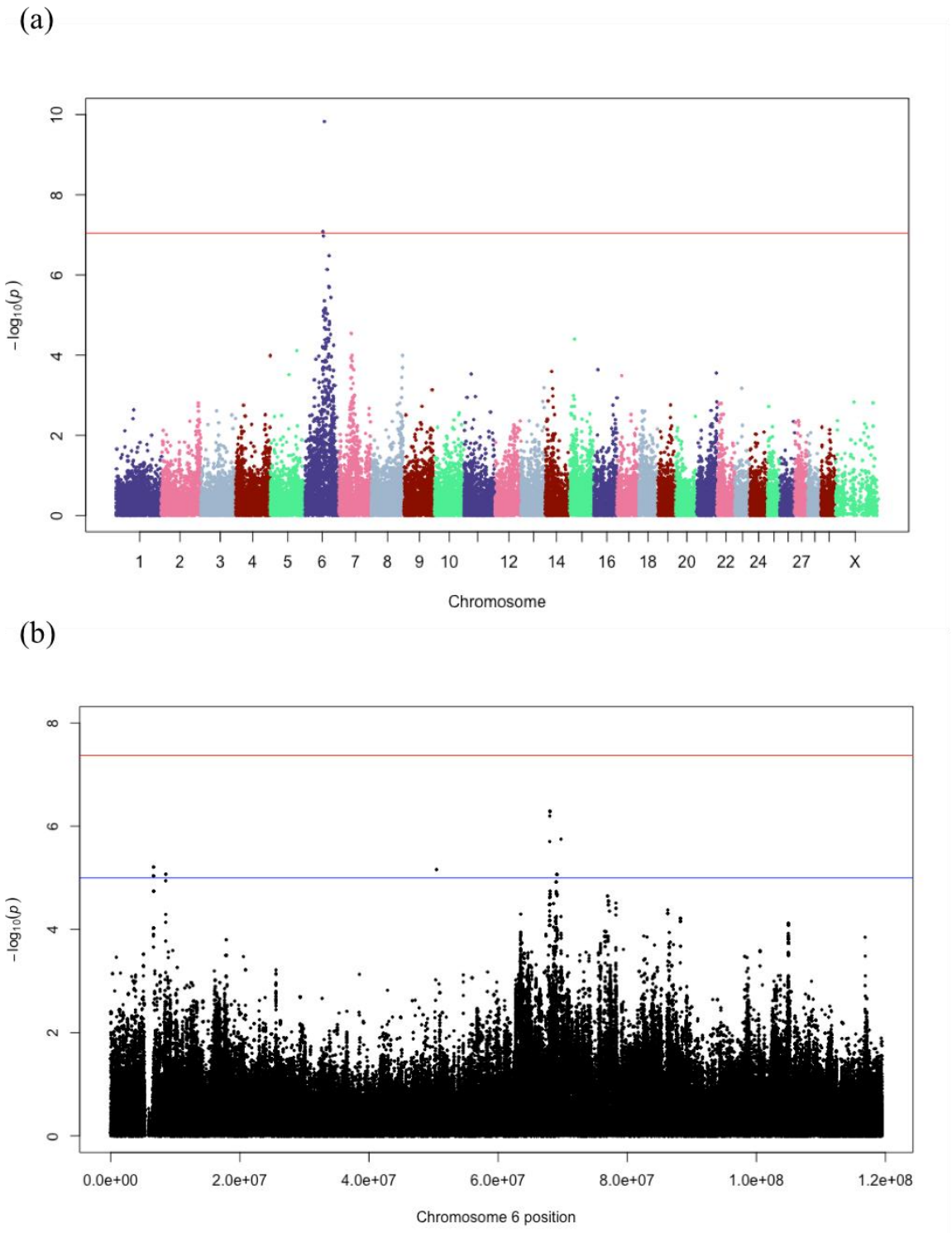

Figure 4. Genome- and chromosome-wide associations for gray vs. not gray. The -$\log_{10}$(P) is plotted for each SNP. The horizontal red line indicates the cutoff for P=0.05 after Bonferroni correction. (a) Genome-wide association using 553,344 SNP genotypes. (b) Chromosome-wide association analysis using 1,177,091 imputed SNP markers. The blue line indicates the default suggestive cutoff at -$\log_{10}$(1e-5). All other SNP meeting this cutoff were intergenic variants.

Remaining consistent with a previous finding within this population (Holland 2015), *CORIN* is the candidate gene associated with the gray phenotype. Atrial natriuretic peptide-converting enzyme is a type II transmembrane serine protease that is expressed primarily in the heart. Functional studies have shown that atrial natriuretic peptide-converting enzyme converts pro-atrial natriuretic peptide (pro-ANP) to mature ANP, a cardiac hormone important in regulating salt-water balance and maintaining normal blood pressure. Additionally, SNPs discovered in human *CORIN* were found to be associated with an increased risk for hypertension and cardiac hypertrophy (Wu 2007). Despite its dominant expression in the heart, recent studies in mice have begun to characterize *CORIN*'s role in melanogenesis. Enshell-Seijffers *et al.* (2008) found it to be normally expressed in the dermal papilla during the anagen (active growth) phase of the hair growth cycle. Loss of atrial natriuretic peptide-converting enzyme causes expansion of the yellow band of pigment within the hair shaft in mice, ultimately resulting in animals with lighter coat color overall. However, its loss was found to have no discernable effect on the expression of other genes associated with coat color such as *ASIP*, *MC1R*, *POMC*, *ATRN*, or *MGRN1* (Enshell-Seijffers et al. 2008). It remains to be seen whether atrial natriuretic peptide-converting enzyme acts via proteolytic processing of a component of the pigment-type switching pathway or via a pathway that antagonizes the response of MC1-R to ASP (Walker & Gunn 2010b).

A 1 Mb region surrounding the lead SNP was extracted from the imputed dataset, and haplotypes were subsequently phased and constructed using fastPHASE (Scheet & Stephens 2006). Exploring the hypothesis that gray has a recessive mode of inheritance, homozygous positions were identified. A series of homozygous SNP surrounding exon 10 were detected,

albeit not surrounding the lead SNP previously identified, with 19 SNP present in intron 10-11 and 20 in intron 9-10 (Fig. 5).

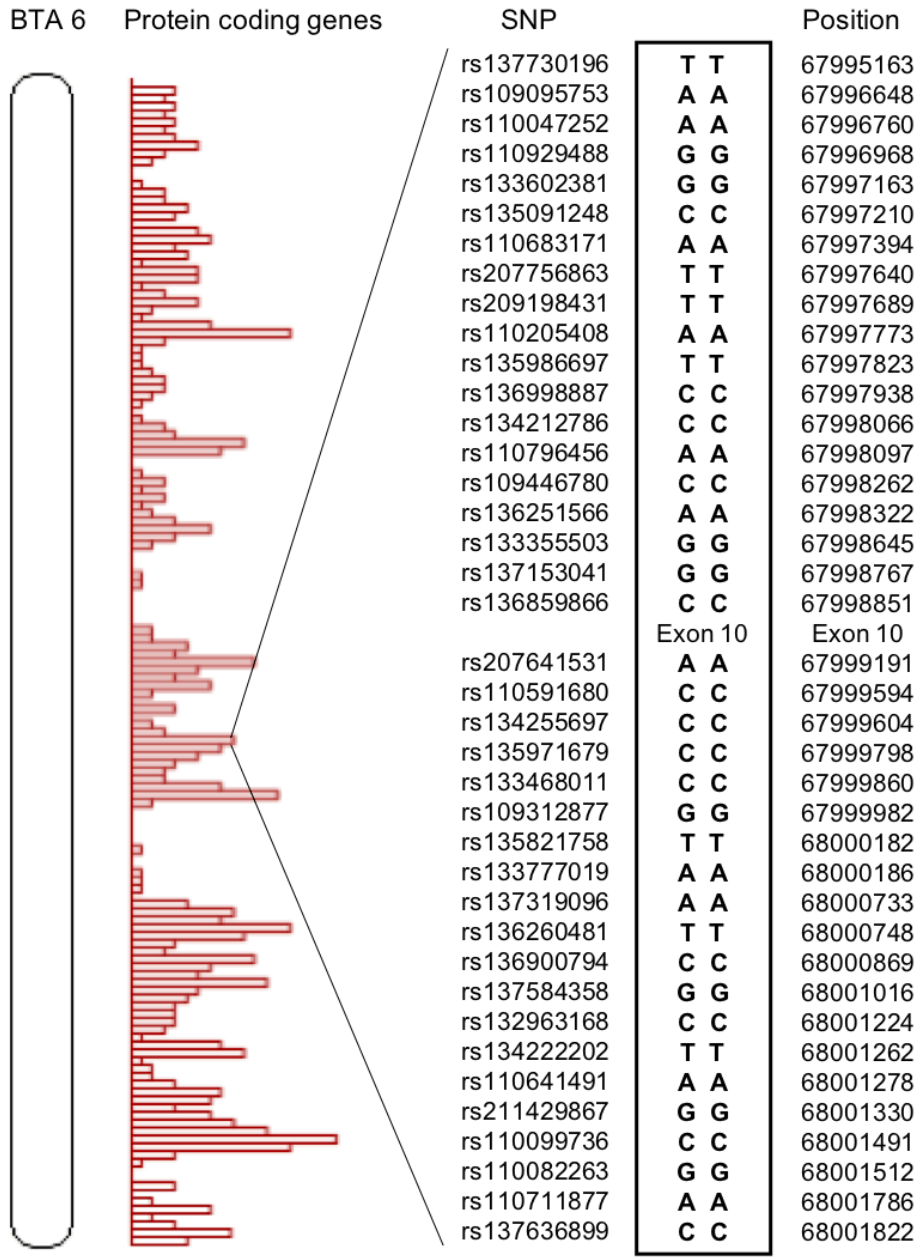

Figure 5. Region of shared homozygosity among gray individuals within *CORIN*. The map position is indicated on the right. Red bars represent the number of protein coding genes within the corresponding chromosomal region.

This region of homozygosity was also found to be present in a subset of other E^+E^+ Cycle 1 individuals that were not gray, but red (Fig. 6). This indicates that these mutations are necessary, but not sufficient, for the gray phenotype. Haplotype breed of origin was tracked through the pedigree to determine if it distinguished the gray individuals from the red E^+E^+ animals harboring the same mutation. All but two gray individuals possessed at least one copy of the Nellore allele at *CORIN*, with 13 being homozygous Nellore and 18 having one copy of both the Nellore and Angus alleles. It is arguable that the two individuals displaying homozygous Angus haplotypes are misclassified, as they appear more red than gray. Breed of origin composition did not largely differ between red and gray animals, although a higher percentage of homozygous Angus animals were observed in the red individuals (Fig. 6). Therefore, breed of origin is clearly influential in the gray individuals, but it does not fully determine their coat color.

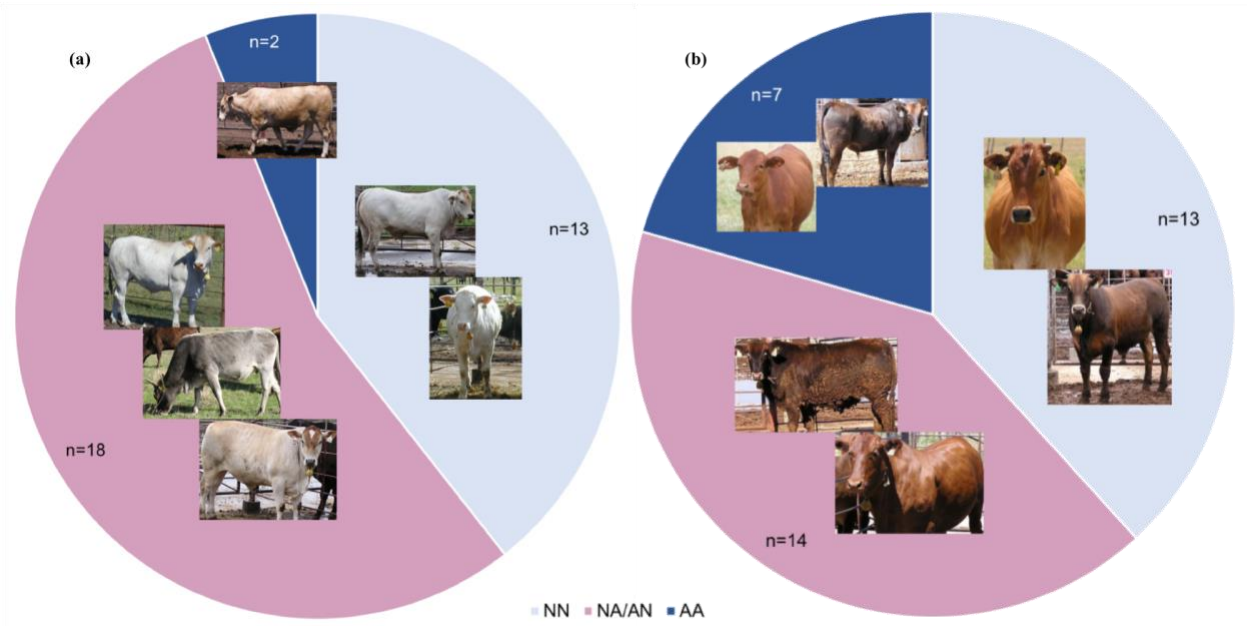

Figure 6. Breed of origin distribution within *CORIN* between (a) gray and (b) non-gray individuals.

Given that the homozygous positions identified in gray individuals are within introns, gray may be the result of a regulatory effect. These introns may contain sequences that bind additional transcriptional enhancers or silencers, albeit not necessarily for *CORIN*, so the mutations can also have an effect on transcription. Introns can also contain sequences of regulatory RNAs (i.e. miRNA, lincRNA) that may affect the translation and stability of the mRNA of *CORIN* and/or other genes. When the mutations change the processing or sequence of these RNAs, varying amounts of gene product can result (Vaz-Drago *et al.* 2017). Another level of regulation applies during splicing. This may be altered when the splicing signals in the introns, where the splice factors bind, are mutated. Mutations in these regions may lead to differentially spliced or truncated products that may not be functional (Vaz-Drago *et al.* 2017).

Alternatively, exon 10 may be affected by these mutations. Exon 10 of *CORIN* encodes a frizzled-like domain, which is closely related to frizzled cysteine-rich domains (Pei & Grishin 2012). Other genes with this same domain include frizzled related protein (*FRZB*) and the frizzled class receptor 1-9 (*FZD1*, *FZD2*, *FZD3*, *FZD4*, *FZD5*, *FZD6*, *FZD7*, *FZD8*, and *FZD9*). Several tyrosine kinase receptors also possess this domain, such as receptor tyrosine kinase like orphan receptor 1 (*ROR1*) and muscle associated receptor tyrosine kinase (*MUSK*). The frizzled class receptors are seven-transmembrane G-protein coupled receptors similar to MC1-R, and act as receptors in the Wnt/β-catenin signaling pathway (Malbon 2004). Wnt is a glycoprotein that has essential roles in development, predominantly through the engagement of Frizzled receptors (Janda *et al.* 2012). When Wnt binds to Frizzled, β-catenin is activated (Hearing & Leong 2006). β-catenin, similar to atrial natriuretic peptide-converting enzyme, is expressed in the dermal papilla of the hair follicle and throughout the growing phase of hair (Enshell-Seijffers *et al.* 2010). β-catenin's activity has also been known to activate atrial natriuretic peptide-converting

enzyme. Mice possessing a complete loss of β-catenin resulted in lighter coat colors than wild-type mice (Enshell-Seijffers *et al.* 2010), suggesting that a defective frizzled-like domain within atrial natriuretic peptide-converting enzyme may be resulting in faulty Wnt signaling within melanogenesis and resulting in β-catenin depletion in gray cattle.

Histological examination of skin and hair was performed to establish how melanocytes and/or melanin distribution is being affected in the gray phenotype. Both H&E and melanin bleach stains demonstrated that gray individuals possess no or extremely little melanin in their hair bulb and shaft, indicating that melanin production is being affected. Figure 7 displays the hair bulbs and shafts of non-gray animals. A normal hair shaft typically has uniform pigmentation (Adya *et al.* 2011), but the gray animals had no melanin reaching the shaft. Further examination of each hair bulb revealed that the melanocytes were the true reason behind the melanin depletion, as they were either not present or misplaced (Fig. 8). Melanocytes in the upper and lower follicular matrix compartments can be separated by the Line of Auber, which is an imaginary line drawn across the widest region of the hair bulb (Liao *et al.* 2017). Melanocytes in the lower matrix are relatively undifferentiated and nonmelanogenic, whereas differentiated, mature and dendritic melanocytes reside in the upper half and produce melanin (Peters *et al.* 2002; Mills 2012). Inactive, or amelanotic, melanocytes can also be present in the outer root sheath. These melanocytes have the potential to become active, but only after injury causes them to migrate into the upper portion of the outer root sheath and to the regenerating epidermis (Mills 2012). Non-gray Nellore-Angus cattle all demonstrated normal, active melanocytes located in the upper half of the follicular matrix. Gray animals, on the other hand, show consistent melanocyte dislocation in either or both the lower follicular matrix and outer root sheath. This improper placement results in no melanin within the hair bulb or shaft of gray animals.

It is important to note, however, that not all of the melanocytes present in gray animals were inactive. H&E staining shows that gray animals have functional epidermal melanocytes, as they display normal and intact skin pigmentation. According to D'Mello *et al.* (2016), epidermal and follicular melanins are independent units, and the co-expression of white hair on highly pigmented skin is a clear affirmation of this. Therefore, gray coat color in Nellore-Angus crossbred cattle is being seen as an optical illusion—gray individuals have no pigmentation within their hair shaft, resulting in white hair, but possess skin pigmentation. The dark skin behind the white hair allows the human eye to perceive the color as gray.

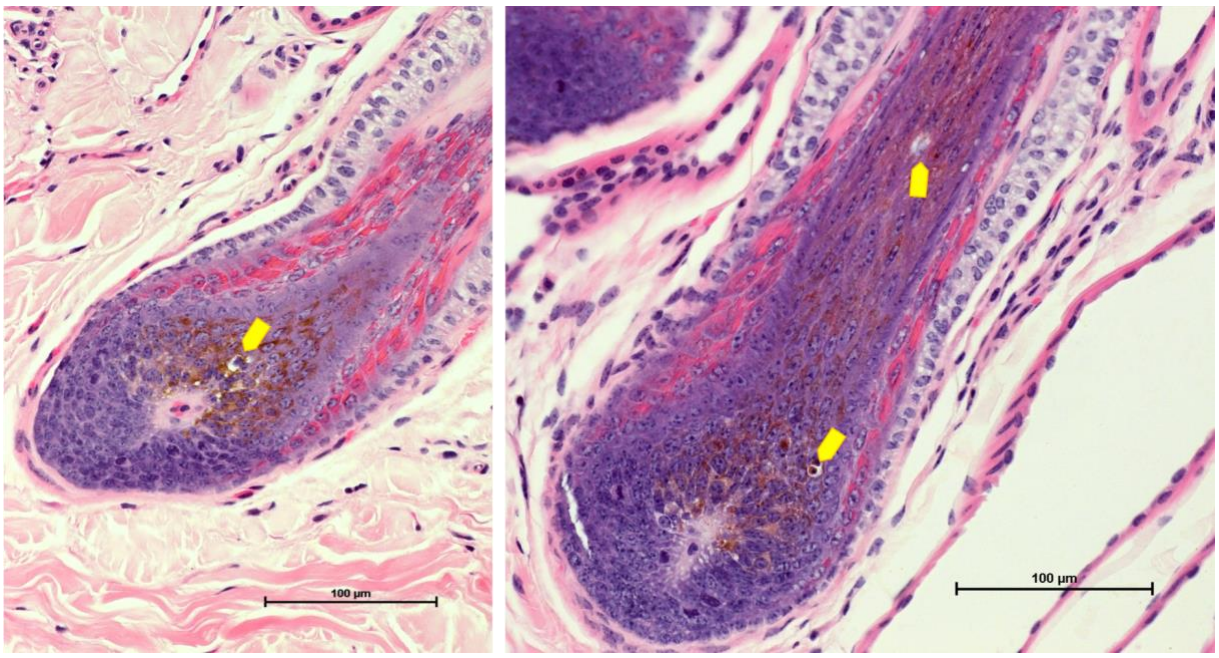

Figure 7. H&E histology for non-gray animals. Yellow arrows point to normally located melanocytes.

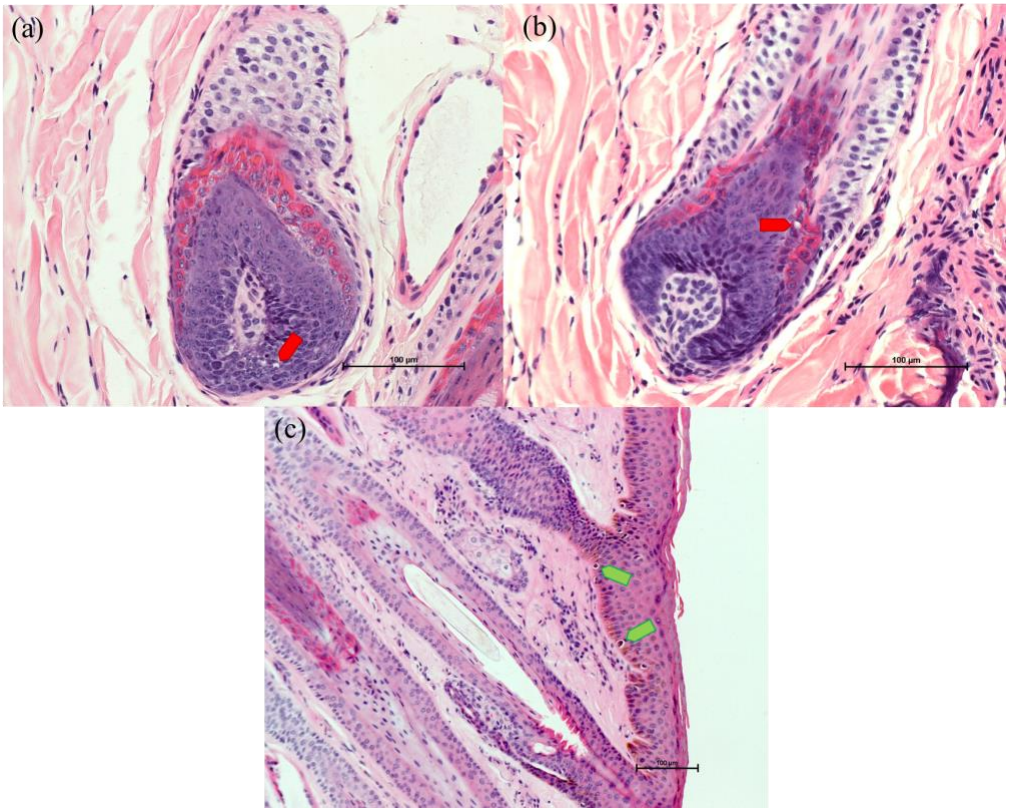

Figure 8. H&E histology for gray animals. No melanin exists in the hair bulbs. (a) The red arrow indicates a melanocyte in the lower matrix of the hair bulb. (b) The red arrow indicates a melanocyte in the outer root sheath. (c) The hair bulb contains no melanocytes, and the hair shaft is unpigmented. Green arrows point to normally located melanocytes in the epidermis.

3.2 Red

The degree of reddening in Nellore-Angus cattle, especially in those possessing E^DE^+ genotypes at *MC1R*, was found to largely depend on the animal's breed of origin at the reddening locus, namely within *CHIC2* (Hanna *et al.* 2014; Womack 2015). With the focus on E^DE^+ red (homozygous Nellore genotypes at *CHIC2*—E^DE^+/NN) (n=3) and E^DE^+ black (homozygous Angus genotypes at *CHIC2*—E^DE^+/AA) (n=3) individuals, *CHIC2* haplotypes were extracted from the imputed high-density dataset (1,177,091 SNP) on BTA 6 and were mined for homozygous positions differing between the two animal groups. A total of 33 homozygous SNP within *CHIC2* were found to differ between the two sets of animals (Table 2).

Table 2. Homozygous SNP within *CHIC2* differing between E^DE^+/homozygous Nellore and E^DE^+/homozygous Angus individuals. All positions are intron variants.

Variant ID	Position (BTA 6)	In EDE+/NN	In EDE+/AA
rs720585423	71188498	TT	AA
rs721197419	71192208	AA	TT
rs526192959	71193711	GG	AA
rs526340776	71196163	TT	CC
rs718317491	71197984	CC	TT
rs437827628	71202264	CC	GG
rs134620307	71202628	CC	TT
rs518805722	71204719	GG	AA
rs515826154	71204983	CC	AA
rs721014809	71208187	CC	TT
rs722930180	71211635	CC	GG
rs721983920	71213788	CC	TT
rs466883267	71213883	TT	CC
rs719382007	71214051	CC	AA
rs479098456	71214397	CC	AA
rs437845692	71216520	CC	TT
rs521948023	71216997	GG	AA
rs723580991	71217109	AA	TT
rs522795348	71217622	GG	AA
rs526579369	71220586	GG	AA
rs714025441	71220732	TT	GG
rs524999571	71223891	GG	AA
rs518625461	71223949	GG	TT
rs715616478	71224424	GG	AA
rs716195077	71226785	AA	GG
rs525976897	71228580	GG	AA
rs474535558	71228836	CC	TT
rs444696595	71229561	GG	AA
rs714303929	71233078	CC	TT
rs463071871	71233626	GG	CC
rs525849908	71233843	CC	TT
rs460520365	71235656	AA	GG
rs449191549	71236815	AA	GG

CHIC2 was extracted and examined in the founders of $E^{D}E^{+}$/NN and $E^{D}E^{+}$/AA individuals. The gene was largely similar between the founders, except for three regions which differed in $E^{D}E^{+}$/NN founders (Fig. 9). A deletion event and missense mutation in exon 3 (g.71213287T>A) were identified, as well as an interchromosomal rearrangement encompassing exon 1 of the gene. Mutations and their corresponding colors were interpreted using the IGV User Guide (Robinson *et al.* 2011). Interchromosomal events are due to unequal crossing over (Dutly & Schinzel 1996). Given these reads are not color coded as being larger or smaller than expected (deletions or insertions, respectively), a translocation event may be occurring in this region. Exon 1 of *CHIC2* encodes a coiled coil. Many coiled coil-type proteins are involved in important biological functions such as the regulation of gene expression (Coletta *et al.* 2010). In spite of this, mutation events within exon 3 are more likely to influence the reddening phenotype.

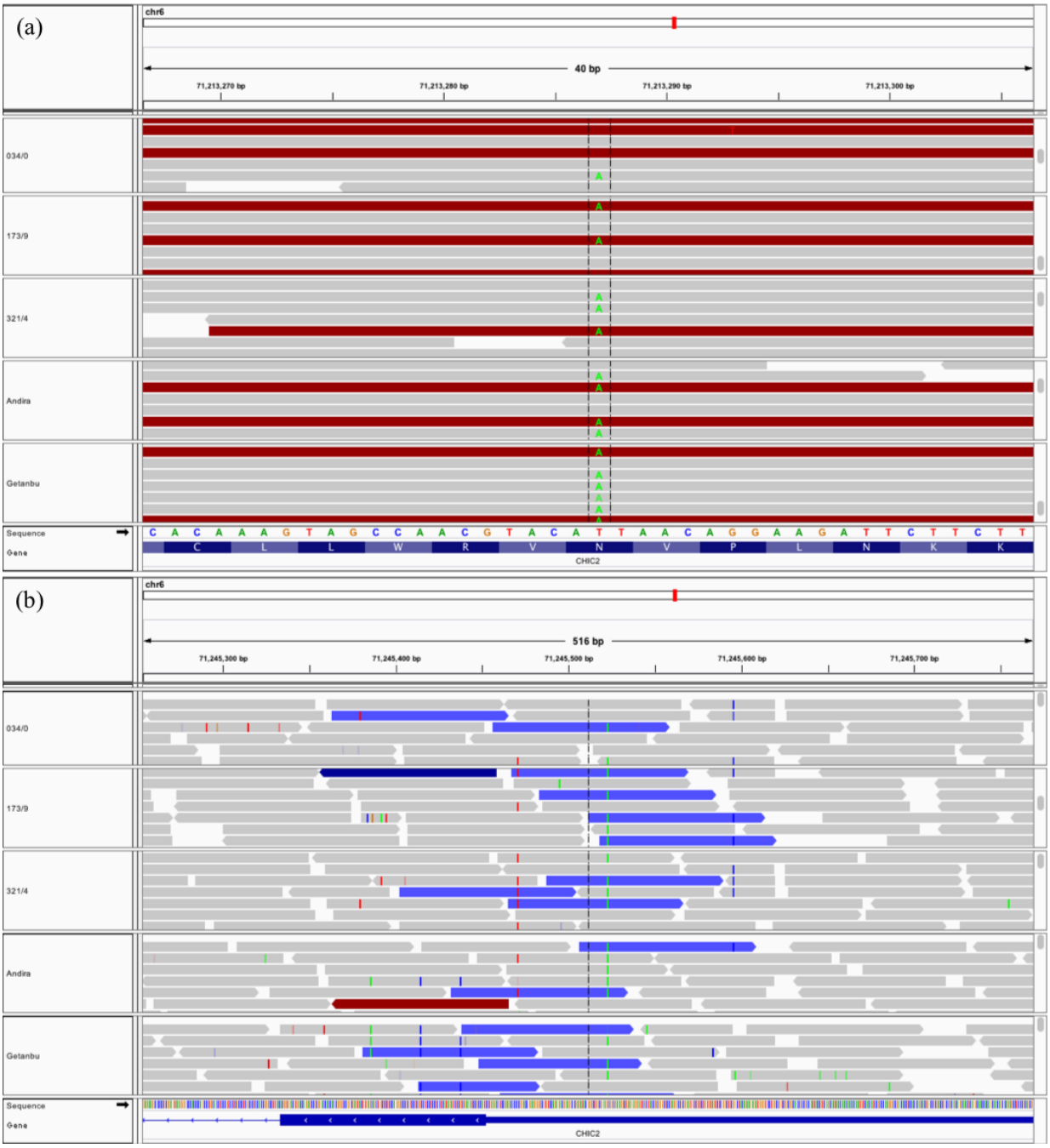

Figure 9. Genomic data of $E^{D}E^{+}$/NN founders. Founder IDs are indicated on the left. (a) Exon 3 of *CHIC2* from 71213270 bp to 71213310 bp. Red reads indicate inferred insert sizes that are larger than expected (deletions). The missense mutation (g.71213287T>A) is outlined and indicated by green text. (b) Blue reads indicate an interchromosomal rearrangement encompassing exon 1 and the 5' UTR of *CHIC2* with read pairs mapping to chromosome 1.

Exon 3 of *CHIC2* represents Golgin subfamily A member 7/ERF4 and also contains the CHIC motif. Golgin subfamily A member 7/ERF4 is involved with protein transport from Golgi to cell surface, or in this case would be transporting melanosomes from the melanocyte to the hair shaft. If a deletion event was occurring within this exon, then the movement of melanin out of the cell could be inactive. Additionally, if the CHIC motif is deleted then palmitoylation is disrupted. Palmitoylation is the covalent attachment of fatty acids, such as palmitic acid, to cysteine residues of proteins which are typically membrane-bound. The cysteine-rich hydrophobic (CHIC) motif was first characterized in human and is a region of amino acids within *CHIC2* where the cysteines are palmitoylated. Cattle possess 100% sequence identity to the human *CHIC2* sequence, and their CHIC motif lies within exon 3. If palmitoylation at this site is disrupted, then CHIC2 would be unable to bind to vesicular structures, namely the melanosome, and therefore would not be able to transfer it and the melanin it contains out of the cell and into the hair shaft. The missense mutation within this exon may be causing a similar scenario in $E^{D}E^{+}$ red individuals, as the mutated SNP occurs prior to the CHIC motif. This missense mutation changes a polar asparagine to a nonpolar isoleucine, which the Sorting Intolerant from Tolerant (SIFT) algorithm (Kumar *et al.* 2009) predicts to be deleterious. This may be truncating the protein prior to the CHIC motif, disrupting palmitoylation and disabling melanin transport.

When compared to melanoregulin (*MREG*), *CHIC2* demonstrates striking similarities. Melanoregulin is a negative regulator of melanosome transfer to keratinocytes (Wu *et al.* 2012). *MREG* can modify its proteins to become membrane-bound upon palmitoylation, exclusively targeting end-stage melanosomes that have already produced pigment (Linder & Deschenes 2007; Wu *et al.* 2012). CHIC2 has also been known to bind to vesicular structures (Cools *et al.*

2001), and largely resembles cysteine string proteins. Melanoregulin possesses many sites for palmitoylation, similar to CHIC2 (Fig. 10), which suggests that it, like other multiply-palmitoylated proteins (i.e. cysteine string proteins), may be stably bound to the melanosome membrane because at any one moment it would usually have at least one attached palmitate group (Wu *et al.* 2012). Moreover, high expression of *MREG* results in a loss of melanin transfer due to the melanosomes no longer localizing at the tips of the melanocyte, but instead gathering near the nucleus (Wu *et al.* 2012). Womack (2015) found that *CHIC2* is upregulated in $E^{D}E^{+}$/NN individuals, which would suggest a similar phenomenon. Given the similarities, we hypothesize CHIC2 to play a role in the transfer of melanosomes to the hair shaft. Therefore, immunohistochemical labeling of CHIC2 was performed to determine its localization.

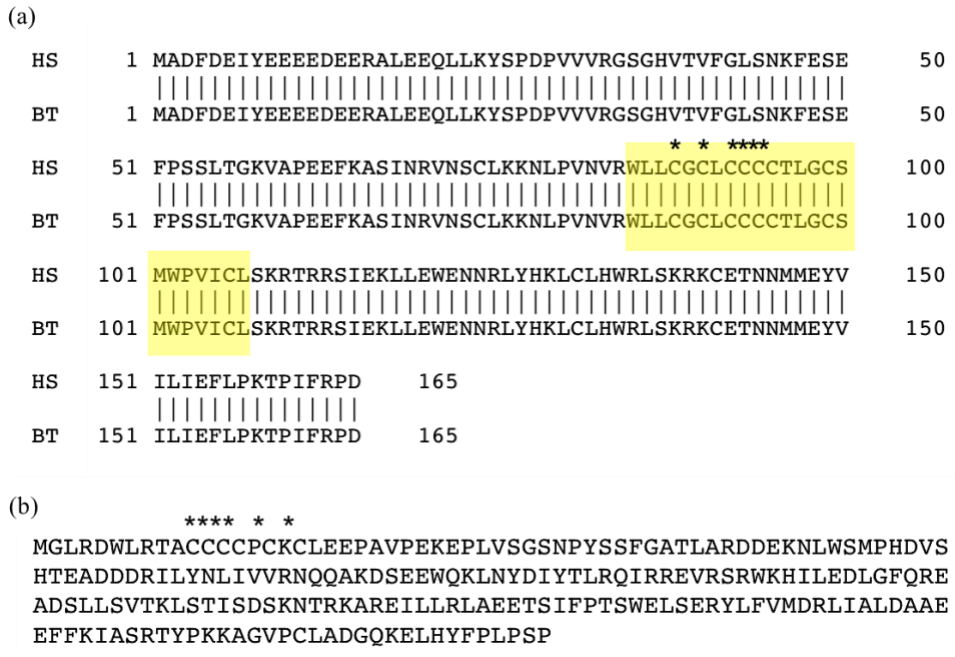

Figure 10. Palmitoylation sites in CHIC2 and MREG. (a) Sequence similarity of CHIC2 between *Homo sapiens* (HS) and *Bos taurus* (BT). The CHIC motif is highlighted, with palmitoylation sites indicated by asterisks. (b) MREG protein sequence. Palmitoylation sites are indicated by asterisks.

A CHIC2 polyclonal antibody with 100% sequence identity with cow was utilized, and DAB was used to stain the protein brown. No differences in IHC were observed between $E^{D}E^{+}$/AA and $E^{D}E^{+}$/NN individuals (Fig. 11). The melanin bleach histology performed on these individuals using no oxalic acid was effective in bleaching out the tissue surrounding the hair bulb, but not the melanin within it. These stains demonstrated unusual similarity to the IHC (Fig. 12). Therefore, it was concluded that the presence of melanin, which also appears brown under a microscope, interfered with IHC binding. If IHC were to be repeated in the future using the same detection method, the melanin would need to be bleached out prior to avoid confounding colors imparted by melanin. Figure 13 depicts different melanin bleach stains. If repeating this experiment, the melanin bleach using 1% oxalic acid and potassium permanganate for one hour (Fig. 13(b)) would be utilized, as it effectively bleaches out the melanin and leaves the tissue largely intact. Alternatively, the immunological localization could be detected using a system not confounded by melanin's presence, either by an enzymatic conjugate that yields a differently colored enzymatically formed precipitate or, perhaps most effectively, a direct or indirect fluorophore localization system.

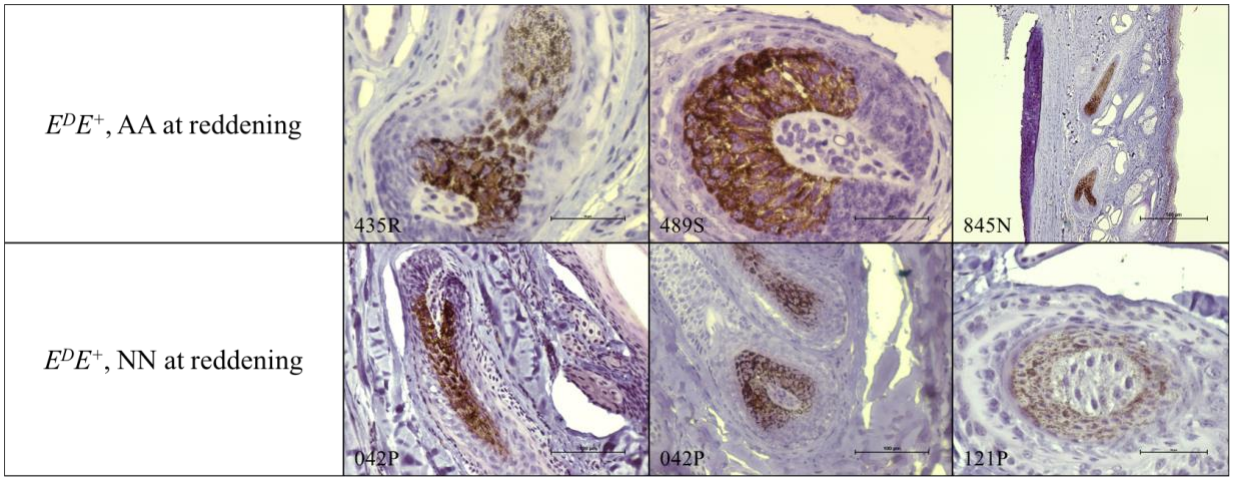

Figure 11. Immunohistochemistry of CHIC2. Animal IDs are listed in the lower left-hand corner.

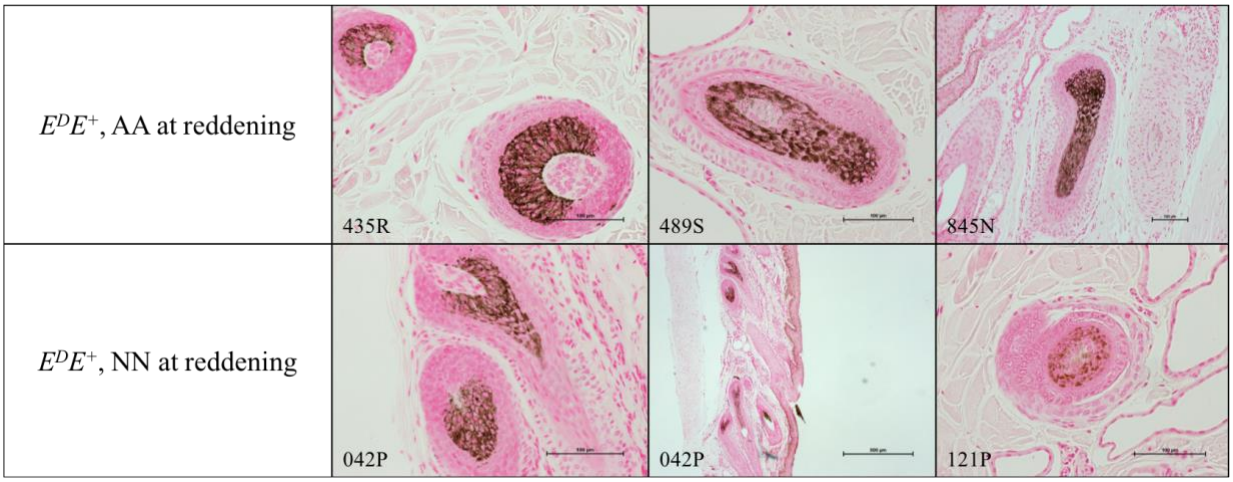

Figure 12. Melanin bleach histology. Melanin bleach stains using no oxalic acid. Animal IDs are listed in the lower left-hand corner.

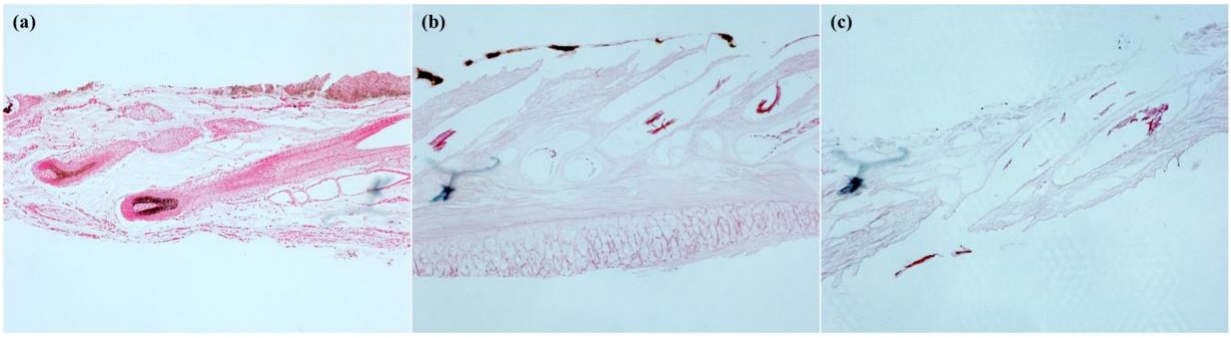

Figure 13. Melanin bleach stain types. (a) Melanin bleach using no oxalic acid. (b) Melanin bleach using 1% oxalic acid and potassium permanganate for one hour. (c) Melanin bleach using 1% oxalic acid and potassium permanganate for two hours.

3.3 White spotted

Three genome-wide association studies using 553,344 SNP genotypes for 560 animals were conducted for (1) spotted (any location) (n=96) vs. not spotted (n=464), (2) facial spots (n=65) vs. no facial spots (n=495), and (3) body spots (n=64) vs. no body spots (n=496), with *MC1R* genotypes fitted as a fixed effect in all three instances (Fig. 14). However, all three *MC1R* genotypes within the herd were represented among spotted animals (E^+E^+=19, E^DE^+=45, E^DE^D=32), and were not unique to face or body spots. A genomic relationship matrix was also integrated into each model. The hypothesis was that spotting would be associated with *KIT*, and the SNPs within *KIT* associated with face and body spots would differ. In cattle, *KIT* is located on BTA 6 at 71796318-71917431 bp. In all three GWAS, the most significant SNP associated with each phenotype was not located within *KIT*. For all spotting, regardless of location, the lead SNP was located on BTA 6 at 72540759 ($P_{raw}=1.26 \times 10^{-23}$, $P_{adjusted}=6.97 \times 10^{-18}$). The most significant SNP associated with face spots was located on BTA 6 at 70792999 bp ($P_{raw}=6.76 \times 10^{-25}$, $P_{adjusted}=3.74 \times 10^{-19}$), whereas the most significant SNP associated with body spots was at 71764979 bp ($P_{raw}=4.30 \times 10^{-24}$, $P_{adjusted}=2.379 \times 10^{-18}$), also on BTA 6. Although none of these

associated markers were positioned directly within *KIT*, they were within 1 Mb of the gene. Each GWAS may have been skewed due to the poor assembly of *KIT*, as seen in the founders (Fig. 15). The reads shown in the founders are dominantly white. This indicates that they were given a mapping quality of zero when aligned with BWA and that the reads are not uniquely mapped. *KIT* is poorly aligned to UMD3.1 in both Nellore and Angus founders beginning at 71798 kb and ending at 71833 kb. Given the close vicinity of each associated SNP to *KIT*, known assembly errors in this region and thus inaccurate imputation, and the existing knowledge of *KIT*'s role in spotting in both cattle and other mammals, the hypothesis that *KIT* is also responsible for white spotting in Nellore-Angus crossbred cattle persists.

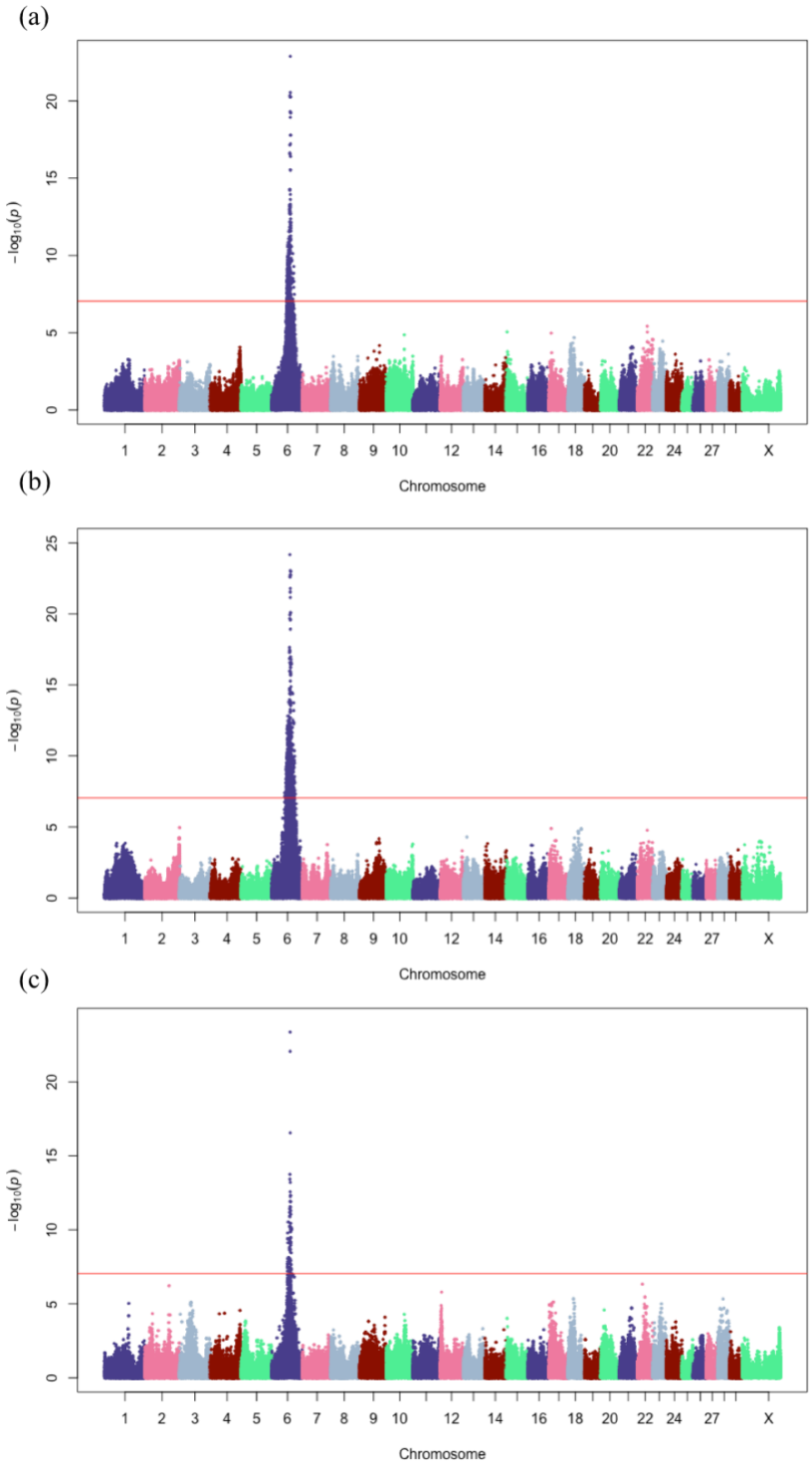

Figure 14. Genome-wide association studies for white spotting. Each GWAS used 553,344 markers. Fitted for genotypes at *MC1R*. The -log$_{10}$(*P*) is plotted for each SNP. The horizontal red line indicates the cutoff for *P*=0.05 after Bonferroni correction. (a) GWAS for spotted vs. not spotted; includes both face and body spots. (b) GWAS for face spots vs. no face spots. (c) GWAS for body spots vs. no body spots. Udder spots were included in this phenotype.

Figure 15. Genomic data of spotted founders. Founder IDs are listed in the left panel. The bottom three individuals (IDs: 099X, 2016, and 2017) represent Angus founders, while the remainder are Nellore.

Haplotypes encompassing *KIT* and a 1 kb region on either side of the gene were extracted. Breed of origin was traced through the pedigree to determine if it plays a role in the spotting phenotype. Although no pattern existed among all spotted individuals, those with only facial spots (but no body spots) (n=32) all possessed at least one copy of the Nellore allele. Breed of origin among those with body spots varied. However, udder spots were considered as body spots, and each of these individuals possessing only udder spots (n=17) had at least one copy of the Angus allele. Individuals possessing both face and body spots (n=33) were homozygous Nellore, except for one individual that was homozygous Angus. However, this individual's spots were more consistent with a roan phenotype as opposed to distinctive spots.

4. CONCLUSION

A 4 Mb region from 67.9 Mb to 71.9 Mb on BTA 6 is involved in coat color determination in Nellore-Angus crossbred cattle. It has been found that this region on BTA 6, coupled with other multilocus influences, is associated with gray, red, and spotted coat color phenotypes in this cross. Haplotype breed of origin was also found to be influential. Histological examination of gray cattle demonstrated that hair and skin color are able to develop through separate avenues given the presence of unpigmented hairs on an otherwise pigmented skin background. A region of homozygous SNP surrounding exon 10 within *CORIN* was identified in gray individuals, although these mutations were found to be necessary but not sufficient for gray. Within *CHIC2*, 33 homozygous positions were identified that differed between red (homozygous Nellore (NN) at *CHIC2*) and non-red (homozygous Angus (AA) at *CHIC2*) $E^{D}E^{+}$ individuals. Whole-genome sequence data was found to be more informative than SNP genotypes alone for the reddening phenotype, as the founders of the $E^{D}E^{+}$/NN individuals revealed both a missense mutation and deletion event within exon 3 that SNP genotypes were unable to capture, indicating that the CHIC motif may be affected in these animals. Genome-wide association analyses of spotting revealed association of the phenotype with *KIT*, similar to previous findings in cattle and other mammals. This work has begun to characterize the color patterns of crossbred cattle that deviate from Mendelian inheritance. Improving the bovine genome assembly, especially on BTA 6, and further genotyping will greatly aid future work in determining the causal mutations for gray, red and spotted coat colors in Nellore-Angus crossbred cattle.

REFERENCES

Abitbol M., Legrand R. & Tiret L. (2014) A missense mutation in melanocortin 1 receptor is associated with the red coat colour in donkeys. *Animal Genetics* **45**, 878-80.

Adya K.A., Inamadar A.C., Palit A., Shivanna R. & Deshmukh N.S. (2011) Light microscopy of the hair: a simple tool to "untangle" hair disorders. *Int J Trichology* **3**, 46-56.

Allison C. (2009) Color Patterns in Crossbred Beef. New Mexico State University, Cooperative Extension Service.

Amsen E.M. (2009) Studies of Proteins that Regulate Melanin Synthesis and Distribution. In: *Department of Biochemistry*. University of Toronto.

Anderson T.M., vonHoldt B.M., Candille S.I., Musiani M., Greco C., Stahler D.R., Smith D.W., Padhukasahasram B., Randi E., Leonard J.A., Bustamante C.D., Ostrander E.A., Tang H., Wayne R.K. & Barsh G.S. (2009) Molecular and evolutionary history of melanism in North American gray wolves. *Science* **323**, 1339-43.

Anistoroaei R., Krogh A.K. & Christensen K. (2013) A frameshift mutation in the LYST gene is responsible for the Aleutian color and the associated Chediak-Higashi syndrome in American mink. *Anim Genet* **44**, 178-83.

Aoki Y., Saint-Germain N., Gyda M., Magner-Fink E., Lee Y.H., Credidio C. & Saint-Jeannet J.P. (2003) Sox10 regulates the development of neural crest-derived melanocytes in Xenopus. *Dev Biol* **259**, 19-33.

Aronesty E. (2011) ea-utils: command line tools for processing biological sequencing data. http://code.google.com/p/ea-utils.

Awasthi Mishra N., Drogemuller C., Jagannathan V., Keller I., Wuthrich D., Bruggmann R., Beck J., Schutz E., Brenig B., Demmel S., Moser S., Signer-Hasler H., Pienkowska-Schelling A., Schelling C., Sande M., Rongen R., Rieder S., Kelsh R.N., Mercader N. & Leeb T. (2017) A structural variant in the 5'-flanking region of the TWIST2 gene affects melanocyte development in belted cattle. *PLoS ONE* **12**, e0180170.

Baranowska Korberg I., Sundstrom E., Meadows J.R., Rosengren Pielberg G., Gustafson U., Hedhammar A., Karlsson E.K., Seddon J., Soderberg A., Vila C., Zhang X., Akesson M., Lindblad-Toh K., Andersson G. & Andersson L. (2014) A simple repeat polymorphism in the MITF-M promoter is a key regulator of white spotting in dogs. *PLoS ONE* **9**, e104363.

Bellone R.R., Holl H., Setaluri V., Devi S., Maddodi N., Archer S., Sandmeyer L., Ludwig A., Foerster D., Pruvost M., Reissmann M., Bortfeldt R., Adelson D.L., Lim S.L., Nelson J., Haase B., Engensteiner M., Leeb T., Forsyth G., Mienaltowski M.J., Mahadevan P., Hofreiter M., Paijmans J.L., Gonzalez-Fortes G., Grahn B. & Brooks S.A. (2013) Evidence for a retroviral insertion in TRPM1 as the cause of congenital stationary night blindness and leopard complex spotting in the horse. *PLoS ONE* **8**, e78280.

Berryere T.G., Schmutz S.M., Schimpf R.J., Cowan C.M. & Potter J. (2003) TYRP1 is associated with dun coat colour in Dexter cattle or how now brown cow? *Animal Genetics* **34**, 169-75.

Brenig B., Beck J., Floren C., Bornemann-Kolatzki K., Wiedemann I., Hennecke S., Swalve H. & Schutz E. (2013) Molecular genetics of coat colour variations in White Galloway and White Park cattle. *Anim Genet* **44**, 450-3.

Brooks S.A. & Bailey E. (2005) Exon skipping in the KIT gene causes a Sabino spotting pattern in horses. *Mamm Genome* **16**, 893-902.

Brooks S.A., Lear T.L., Adelson D.L. & Bailey E. (2007) A chromosome inversion near the KIT gene and the Tobiano spotting pattern in horses. *Cytogenet Genome Res* **119**, 225-30.

Brunberg E., Andersson L., Cothran G., Sandberg K., Mikko S. & Lindgren G. (2006) A missense mutation in PMEL17 is associated with the Silver coat color in the horse. *BMC Genet* **7**, 46.

Candille S.I., Kaelin C.B., Cattanach B.M., Yu B., Thompson D.A., Nix M.A., Kerns J.A., Schmutz S.M., Millhauser G.L. & Barsh G.S. (2007) A -defensin mutation causes black coat color in domestic dogs. *Science* **318**, 1418-23.

Cantanhede I.G. & de Oliveira J.R.M. (2017) PDGF Family Expression in Glioblastoma Multiforme: Data Compilation from Ivy Glioblastoma Atlas Project Database. *Sci Rep* **7**, 15271.

Capomaccio S., Milanesi M., Nocelli C., Giontella A., Verini-Supplizi A., Branca M., Silvestrelli M. & Cappelli K. (2017) Splicing site disruption in the KIT gene as strong candidate for white dominant phenotype in an Italian Trotter. *Anim Genet* **48**, 727-8.

Charlier C., Denys B., Belanche J.I., Coppieters W., Grobet L., Mni M., Womack J., Hanset R. & Georges M. (1996) Microsatellite mapping of the bovine roan locus: a major determinant of White Heifer disease. *Mamm Genome* **7**, 138-42.

Cheung M. & Briscoe J. (2003) Neural crest development is regulated by the transcription factor Sox9. *Development* **130**, 5681-93.

Choi T.J., Lee S.S., Yoon D.H., Kang H.S., Kim C.D., Hwang I.H., Kim C.Y., Jin X., Yang C.G. & Seo K.S. (2012) Determination of Genetic Diversity among Korean Hanwoo Cattle Based on Physical Characteristics. *Asian-Australas J Anim Sci* **25**, 1205-15.

Cock P.J., Fields C.J., Goto N., Heuer M.L. & Rice P.M. (2010) The Sanger FASTQ file format for sequences with quality scores, and the Solexa/Illumina FASTQ variants. *Nucleic Acids Res* **38**, 1767-71.

Coletta A., Pinney J.W., Solis D.Y., Marsh J., Pettifer S.R. & Attwood T.K. (2010) Low-complexity regions within protein sequences have position-dependent roles. *Bmc Systems Biology* **4**, 43.

Cools J., Mentens N. & Marynen P. (2001) A new family of small, palmitoylated, membrane-associated proteins, characterized by the presence of a cysteine-rich hydrophobic motif. *Febs Letters* **492**, 204-9.

D'Mello S.A., Finlay G.J., Baguley B.C. & Askarian-Amiri M.E. (2016) Signaling Pathways in Melanogenesis. *International Journal of Molecular Sciences* **17**.

da Silva R.G., La Scala N. & Tonhati H. (2003) Radiative properties of the skin and haircoat of cattle and other animals. *Transactions of the Asae* **46**, 913-8.

David V.A., Menotti-Raymond M., Wallace A.C., Roelke M., Kehler J., Leighty R., Eizirik E., Hannah S.S., Nelson G., Schaffer A.A., Connelly C.J., O'Brien S.J. & Ryugo D.K. (2014) Endogenous retrovirus insertion in the KIT oncogene determines white and white spotting in domestic cats. *G3 (Bethesda)* **4**, 1881-91.

DePristo M.A., Banks E., Poplin R., Garimella K.V., Maguire J.R., Hartl C., Philippakis A.A., del Angel G., Rivas M.A., Hanna M., McKenna A., Fennell T.J., Kernytsky A.M., Sivachenko A.Y., Cibulskis K., Gabriel S.B., Altshuler D. & Daly M.J. (2011) A

framework for variation discovery and genotyping using next-generation DNA sequencing data. *Nature Genetics* **43**, 491-+.

Dikmen S., Dahl G.E., Cole J.B., Null D.J. & Hansen P.J. (2017) The Larson Blue coat color phenotype in Holsteins: Characteristics and effects on body temperature regulation and production in lactating cows in a hot climate. *J Anim Sci* **95**, 1164-9.

Dorshorst B., Henegar C., Liao X., Sallman Almen M., Rubin C.J., Ito S., Wakamatsu K., Stothard P., Van Doormaal B., Plastow G., Barsh G.S. & Andersson L. (2015) Dominant Red Coat Color in Holstein Cattle Is Associated with a Missense Mutation in the Coatomer Protein Complex, Subunit Alpha (COPA) Gene. *PLoS ONE* **10**, e0128969.

Dreger D.L. & Schmutz S.M. (2010) The variant red coat colour phenotype of Holstein cattle maps to BTA27. *Anim Genet* **41**, 109-12.

Drogemuller C., Engensteiner M., Moser S., Rieder S. & Leeb T. (2009) Genetic mapping of the belt pattern in Brown Swiss cattle to BTA3. *Anim Genet* **40**, 225-9.

Dunn K.J., Brady M., Ochsenbauer-Jambor C., Snyder S., Incao A. & Pavan W.J. (2005) WNT1 and WNT3a promote expansion of melanocytes through distinct modes of action. *Pigment Cell Res* **18**, 167-80.

Durig N., Jude R., Holl H., Brooks S.A., Lafayette C., Jagannathan V. & Leeb T. (2017) Whole genome sequencing reveals a novel deletion variant in the KIT gene in horses with white spotted coat colour phenotypes. *Anim Genet* **48**, 483-5.

Durkin K., Coppieters W., Drogemuller C., Ahariz N., Cambisano N., Druet T., Fasquelle C., Haile A., Horin P., Huang L., Kamatani Y., Karim L., Lathrop M., Moser S., Oldenbroek K., Rieder S., Sartelet A., Solkner J., Stalhammar H., Zelenika D., Zhang Z., Leeb T.,

Georges M. & Charlier C. (2012) Serial translocation by means of circular intermediates underlies colour sidedness in cattle. *Nature* **482**, 81-4.

Dutly F. & Schinzel A. (1996) Unequal interchromosomal rearrangements may result in elastin gene deletions causing the Williams-Beuren syndrome. *Human Molecular Genetics* **5**, 1893-8.

Enshell-Seijffers D., Lindon C. & Morgan B.A. (2008) The serine protease Corin is a novel modifier of the Agouti pathway. *Development* **135**, 217-25.

Enshell-Seijffers D., Lindon C., Wu E., Taketo M.M. & Morgan B.A. (2010) Beta-catenin activity in the dermal papilla of the hair follicle regulates pigment-type switching. *Proc Natl Acad Sci U S A* **107**, 21564-9.

Fan Y., Wang P., Fu W., Dong T., Qi C., Liu L., Guo G., Li C., Cui X., Zhang S., Zhang Q., Zhang Y. & Sun D. (2014) Genome-wide association study for pigmentation traits in Chinese Holstein population. *Anim Genet* **45**, 740-4.

Fang M., Larson G., Ribeiro H.S., Li N. & Andersson L. (2009) Contrasting mode of evolution at a coat color locus in wild and domestic pigs. *Plos Genetics* **5**, e1000341.

Fontanesi L., Beretti F., Riggio V., Gomez Gonzalez E., Dall'Olio S., Davoli R., Russo V. & Portolano B. (2009) Copy number variation and missense mutations of the agouti signaling protein (ASIP) gene in goat breeds with different coat colors. *Cytogenet Genome Res* **126**, 333-47.

Fontanesi L., D'Alessandro E., Scotti E., Liotta L., Crovetti A., Chiofalo V. & Russo V. (2010a) Genetic heterogeneity and selection signature at the KIT gene in pigs showing different coat colours and patterns. *Anim Genet* **41**, 478-92.

Fontanesi L., Scotti E., Allain D. & Dall'olio S. (2014) A frameshift mutation in the melanophilin gene causes the dilute coat colour in rabbit (Oryctolagus cuniculus) breeds. *Anim Genet* **45**, 248-55.

Fontanesi L., Scotti E. & Russo V. (2012) Haplotype variability in the bovine MITF gene and association with piebaldism in Holstein and Simmental cattle breeds. *Anim Genet* **43**, 250-6.

Fontanesi L., Tazzoli M., Beretti F. & Russo V. (2006) Mutations in the melanocortin 1 receptor (MC1R) gene are associated with coat colours in the domestic rabbit (Oryctolagus cuniculus). *Anim Genet* **37**, 489-93.

Fontanesi L., Tazzoli M., Russo V. & Beever J. (2010b) Genetic heterogeneity at the bovine KIT gene in cattle breeds carrying different putative alleles at the spotting locus. *Anim Genet* **41**, 295-303.

Gerding W.M., Akkad D.A. & Epplen J.T. (2013) Spotted Weimaraner dog due to de novo KIT mutation. *Anim Genet* **44**, 605-6.

Gill C.A. (2016) Genomic imputation of a multigenerational Nellore-Angus mapping population. *Journal of Animal Science* **94**, 15-.

Girardot M., Guibert S., Laforet M.P., Gallard Y., Larroque H. & Oulmouden A. (2006) The insertion of a full-length Bos taurus LINE element is responsible for a transcriptional deregulation of the Normande Agouti gene. *Pigment Cell Res* **19**, 346-55.

Gray K.A., Yates B., Seal R.L., Wright M.W. & Bruford E.A. (2015) Genenames.org: the HGNC resources in 2015. *Nucleic Acids Research*, D1079-D85.

Grosz M.D. & MacNeil M.D. (1999) The "spotted" locus maps to bovine chromosome 6 in a Hereford-Cross population. *J Hered* **90**, 233-6.

Gustafson N.A., Gandolfi B. & Lyons L.A. (2017) Not another type of potato: MC1R and the russet coloration of Burmese cats. *Anim Genet* **48**, 116-20.

Gutierrez-Gil B., Wiener P. & Williams J.L. (2007) Genetic effects on coat colour in cattle: dilution of eumelanin and phaeomelanin pigments in an F2-Backcross Charolais x Holstein population. *BMC Genet* **8**, 56.

Haase B., Brooks S.A., Tozaki T., Burger D., Poncet P.A., Rieder S., Hasegawa T., Penedo C. & Leeb T. (2009) Seven novel KIT mutations in horses with white coat colour phenotypes. *Anim Genet* **40**, 623-9.

Haase B., Rieder S. & Leeb T. (2015) Two variants in the KIT gene as candidate causative mutations for a dominant white and a white spotting phenotype in the donkey. *Anim Genet* **46**, 321-4.

Hager J., Dina C., Francke S., Dubois S., Houari M., Vatin V., Vaillant E., Lorentz N., Basdevant A., Clement K., Guy-Grand B. & Froguel P. (1998) A genome-wide scan for human obesity genes reveals a major susceptibility locus on chromosome 10. *Nat Genet* **20**, 304-8.

Han J.L., Yang M., Yue Y.J., Guo T.T., Liu J.B., Niu C.E. & Yang B.H. (2015) Analysis of agouti signaling protein (ASIP) gene polymorphisms and association with coat color in Tibetan sheep (Ovis aries). *Genet Mol Res* **14**, 1200-9.

Han S.-H., Cho I.-C., Kim J.-H., Ko M.-S., Kim Y.-H., Kim E.-Y., Park S.-P. & Lee S.-S. (2011) Coat Color Patterns and Genotypes of Extension and Agouti in Hanwoo and Jeju Black Cattle. *Journal of Life Science* **21**, 494-501.

Hanna L.L.H., Sanders J.O., Riley D.G., Abbey C.A. & Gill C.A. (2014) Identification of a major locus interacting with MC1R and modifying black coat color in an F-2 Nellore-Angus population. *Genetics Selection Evolution* **46**.

Harris R.B., Zhou J., Shi M., Redmann S., Mynatt R.L. & Ryan D.H. (2001) Overexpression of agouti protein and stress responsiveness in mice. *Physiology & Behavior* **73**, 599-608.

Hauswirth R., Haase B., Blatter M., Brooks S.A., Burger D., Drogemuller C., Gerber V., Henke D., Janda J., Jude R., Magdesian K.G., Matthews J.M., Poncet P.A., Svansson V., Tozaki T., Wilkinson-White L., Penedo M.C., Rieder S. & Leeb T. (2012) Mutations in MITF and PAX3 cause "splashed white" and other white spotting phenotypes in horses. *Plos Genetics* **8**, e1002653.

Hauswirth R., Jude R., Haase B., Bellone R.R., Archer S., Holl H., Brooks S.A., Tozaki T., Penedo M.C., Rieder S. & Leeb T. (2013) Novel variants in the KIT and PAX3 genes in horses with white-spotted coat colour phenotypes. *Anim Genet* **44**, 763-5.

He S.J., Stevens G., Braithwaite A.W. & Eccles M.R. (2005) Transfection of melanoma cells with antisense PAX3 oligonucleotides additively complements cisplatin-induced cytotoxicity. *Molecular Cancer Therapeutics* **4**, 996-1003.

Hearing V.J. & Leong S.P. (2006) *From Melanocytes to Melanoma*. Humana Press.

Hecht B.C. (2006) Sequence Analysis of Pmel17 as Candidate Gene for Causing Rat-tail Syndrome in Cattle. In: *Department of Plant and Animal Sciences*. Brigham Young University, BYU ScholarsArchive.

Hida T., Wakamatsu K., Sviderskaya E.V., Donkin A.J., Montoliu L., Lynn Lamoreux M., Yu B., Millhauser G.L., Ito S., Barsh G.S., Jimbow K. & Bennett D.C. (2009) Agouti

protein, mahogunin, and attractin in pheomelanogenesis and melanoblast-like alteration of melanocytes: a cAMP-independent pathway. *Pigment Cell Melanoma Res* **22**, 623-34.

Holl H., Isaza R., Mohamoud Y., Ahmed A., Almathen F., Youcef C., Gaouar S., Antczak D.F. & Brooks S. (2017a) A Frameshift Mutation in KIT is Associated with White Spotting in the Arabian Camel. *Genes (Basel)* **8**.

Holl H.M., Brooks S.A., Carpenter M.L., Bustamante C.D. & Lafayette C. (2017b) A novel splice mutation within equine KIT and the W15 allele in the homozygous state lead to all white coat color phenotypes. *Anim Genet* **48**, 497-8.

Holland P.W. (2015) Identification of the regions of the bovine genome associated with gray coat color in a Nellore-Angus cross population. In: *Animal Sciences*, p. 46. Texas A&M University.

Hou L., Arnheiter H. & Pavan W.J. (2006) Interspecies difference in the regulation of melanocyte development by SOX10 and MITF. *Proc Natl Acad Sci U S A* **103**, 9081-5.

Hubbard J.K., Uy J.A., Hauber M.E., Hoekstra H.E. & Safran R.J. (2010) Vertebrate pigmentation: from underlying genes to adaptive function. *Trends in Genetics* **26**, 231-9.

Ishida Y., David V.A., Eizirik E., Schaffer A.A., Neelam B.A., Roelke M.E., Hannah S.S., O'Brien S.J. & Menotti-Raymond M. (2006) A homozygous single-base deletion in MLPH causes the dilute coat color phenotype in the domestic cat. *Genomics* **88**, 698-705.

Ito S. & Wakamatsu K. (2008) Chemistry of mixed melanogenesis--pivotal roles of dopaquinone. *Photochemistry and Photobiology* **84**, 582-92.

Jacobs L.N., Staiger E.A., Albright J.D. & Brooks S.A. (2016) The MC1R and ASIP Coat Color Loci May Impact Behavior in the Horse. *J Hered* **107**, 214-9.

Janda C.Y., Waghray D., Levin A.M., Thomas C. & Garcia K.C. (2012) Structural basis of Wnt recognition by Frizzled. *Science* **337**, 59-64.

Jin E.J., Erickson C.A., Takada S. & Burrus L.W. (2001) Wnt and BMP signaling govern lineage segregation of melanocytes in the avian embryo. *Dev Biol* **233**, 22-37.

Kanehisa M., Furumichi M., Tanabe M., Sato Y. & Morishima K. (2017) KEGG: new perspectives on genomes, pathways, diseases and drugs. *Nucleic Acids Research* **45**, D353-D61.

Kanehisa M. & Goto S. (2000) KEGG: Kyoto Encyclopedia of Genes and Genomes. *Nucleic Acids Research* **28**, 27-30.

Kanehisa M., Sato Y., Kawashima M., Furumichi M. & Tanabe M. (2016) KEGG as a reference resource for gene and protein annotation. *Nucleic Acids Research* **44**, D457-D62.

Kavar T., Ceh E. & Dovc P. (2012) A simplified PCR-based method for detection of gray coat color allele in horse. *Mol Cell Probes* **26**, 256-8.

Klungland H., Vage D.I., Gomez-Raya L., Adalsteinsson S. & Lien S. (1995) The role of melanocyte-stimulating hormone (MSH) receptor in bovine coat color determination. *Mamm Genome* **6**, 636-9.

Kuhn C. & Weikard R. (2007) An investigation into the genetic background of coat colour dilution in a Charolais x German Holstein F2 resource population. *Anim Genet* **38**, 109-13.

Kuklin A.I., Mynatt R.L., Klebig M.L., Kiefer L.L., Wilkison W.O., Woychik R.P. & Michaud E.J. (2004) Liver-specific expression of the agouti gene in transgenic mice promotes liver carcinogenesis in the absence of obesity and diabetes. *Molecular Cancer* **3**, 17.

Kumar P., Henikoff S. & Ng P.C. (2009) Predicting the effects of coding non-synonymous variants on protein function using the SIFT algorithm. *Nature Protocols* **4**, 1073-82.

Lehner S., Gahle M., Dierks C., Stelter R., Gerber J., Brehm R. & Distl O. (2013) Two-exon skipping within MLPH is associated with coat color dilution in rabbits. *PLoS ONE* **8**, e84525.

Levy C., Khaled M. & Fisher D.E. (2006) MITF: master regulator of melanocyte development and melanoma oncogene. *Trends in Molecular Medicine* **12**, 406-14.

Li H. & Durbin R. (2009) Fast and accurate short read alignment with Burrows-Wheeler transform. *Bioinformatics* **25**, 1754-60.

Li H., Handsaker B., Wysoker A., Fennell T., Ruan J., Homer N., Marth G., Abecasis G., Durbin R. & Genome Project Data Processing S. (2009) The Sequence Alignment/Map format and SAMtools. *Bioinformatics* **25**, 2078-9.

Li W., Sartelet A., Tamma N., Coppieters W., Georges M. & Charlier C. (2016) Reverse genetic screen for loss-of-function mutations uncovers a frameshifting deletion in the melanophilin gene accountable for a distinctive coat color in Belgian Blue cattle. *Anim Genet* **47**, 110-3.

Liao C.P., Booker R.C., Morrison S.J. & Le L.Q. (2017) Identification of hair shaft progenitors that create a niche for hair pigmentation. *Genes Dev* **31**, 744-56.

Linder M.E. & Deschenes R.J. (2007) Palmitoylation: policing protein stability and traffic. *Nat Rev Mol Cell Biol* **8**, 74-84.

Liu L., Harris B., Keehan M. & Zhang Y. (2009) Genome scan for the degree of white spotting in dairy cattle. *Anim Genet* **40**, 975-7.

Malbon C.C. (2004) Frizzleds: new members of the superfamily of G-protein-coupled receptors. *Front Biosci* **9**, 1048-58.

Marklund L., Moller M.J., Sandberg K. & Andersson L. (1996) A missense mutation in the gene for melanocyte-stimulating hormone receptor (MC1R) is associated with the chestnut coat color in horses. *Mammalian Genome* **7**, 895-9.

McKenna A., Hanna M., Banks E., Sivachenko A., Cibulskis K., Kernytsky A., Garimella K., Altshuler D., Gabriel S., Daly M. & DePristo M.A. (2010) The Genome Analysis Toolkit: a MapReduce framework for analyzing next-generation DNA sequencing data. *Genome Research* **20**, 1297-303.

Mills S.E. (2012) *Histology for Pathologists*. Lippincott Williams & Wilkins, Philadelphia, PA.

Negro S., Imsland F., Valera M., Molina A., Sole M. & Andersson L. (2017) Association analysis of KIT, MITF, and PAX3 variants with white markings in Spanish horses. *Anim Genet* **48**, 349-52.

Nonneman D., Shibuya H. & Johnson G.S. (1996) A BstUI PCR/RFLP in the bovine tyrosinase-related protein-1 (TYRP1) gene. *Anim Genet* **27**, 218-9.

Oetting W.S. (2000) The tyrosinase gene and oculocutaneous albinism type 1 (OCA1): A model for understanding the molecular biology of melanin formation. *Pigment Cell Res* **13**, 320-5.

Ohbayashi N., Maruta Y., Ishida M. & Fukuda M. (2012) Melanoregulin regulates retrograde melanosome transport through interaction with the RILP-p150Glued complex in melanocytes. *Journal of Cell Science* **125**, 1508-18.

Olson T. (1999) Genetics of colour variation. *The Genetics of cattle*, 33-53.

Pardanani A., Ketterling R.P., Brockman S.R., Flynn H.C., Paternoster S.F., Shearer B.M., Reeder T.L., Li C.Y., Cross N.C., Cools J., Gilliland D.G., Dewald G.W. & Tefferi A. (2003) CHIC2 deletion, a surrogate for FIP1L1-PDGFRA fusion, occurs in systemic mastocytosis associated with eosinophilia and predicts response to imatinib mesylate therapy. *Blood* **102**, 3093-6.

Pawelek J.M. & Korner A.M. (1982) The biosynthesis of mammalian melanin. *Am Sci* **70**, 136-45.

Pei J. & Grishin N.V. (2012) Cysteine-rich domains related to Frizzled receptors and Hedgehog-interacting proteins. *Protein Science* **21**, 1172-84.

Perez-Guisado J., Lopez-Rodriguez R. & Munoz-Serrano A. (2006) Heritability of dominant-aggressive behaviour in English Cocker Spaniels. *Applied Animal Behaviour Science* **100**, 219-27.

Peters E.M., Tobin D.J., Botchkareva N., Maurer M. & Paus R. (2002) Migration of melanoblasts into the developing murine hair follicle is accompanied by transient c-Kit expression. *Journal of Histochemistry & Cytochemistry* **50**, 751-66.

Peterschmitt M., Grain F., Arnaud B., Deleage G. & Lambert V. (2009) Mutation in the melanocortin 1 receptor is associated with amber colour in the Norwegian Forest Cat. *Anim Genet* **40**, 547-52.

Philipp U., Hamann H., Mecklenburg L., Nishino S., Mignot E., Gunzel-Apel A.R., Schmutz S.M. & Leeb T. (2005) Polymorphisms within the canine MLPH gene are associated with dilute coat color in dogs. *BMC Genet* **6**, 34.

Philipp U., Lupp B., Momke S., Stein V., Tipold A., Eule J.C., Rehage J. & Distl O. (2011) A MITF mutation associated with a dominant white phenotype and bilateral deafness in German Fleckvieh cattle. *PLoS ONE* **6**, e28857.

Phillips G. (2017) Weekly genetics review: What's driving the fashion in black cattle? , Beef Central.

Purcell S., Neale B., Todd-Brown K., Thomas L., Ferreira M.A.R., Bender D., Maller J., Sklar P., de Bakker P.I.W., Daly M.J. & Sham P.C. (2007) PLINK: A tool set for whole-genome association and population-based linkage analyses. *American Journal of Human Genetics* **81**, 559-75.

Rapley E.A., Turnbull C., Al Olama A.A., Dermitzakis E.T., Linger R., Huddart R.A., Renwick A., Hughes D., Hines S., Seal S., Morrison J., Nsengimana J., Deloukas P., Collaboration U.K.T.C., Rahman N., Bishop D.T., Easton D.F. & Stratton M.R. (2009) A genome-wide association study of testicular germ cell tumor. *Nat Genet* **41**, 807-10.

Reinsch N., Thomsen H., Xu N., Brink M., Looft C., Kalm E., Brockmann G.A., Grupe S., Kuhn C., Schwerin M., Leyhe B., Hiendleder S., Erhardt G., Medjugorac I., Russ I., Forster M., Reents R. & Averdunk G. (1999) A QTL for the degree of spotting in cattle shows synteny with the KIT locus on chromosome 6. *Journal of Heredity* **90**, 629-34.

Reissmann M. & Ludwig A. (2013) Pleiotropic effects of coat colour-associated mutations in humans, mice and other mammals. *Semin Cell Dev Biol* **24**, 576-86.

Riley D.G., Welsh T.H., Gill C.A., Hulsman L.L., Herring A.D., Riggs P.K., Sawyer J.E. & Sanders J.O. (2013) Whole genome association of SNP with newborn calf cannon bone length. *Livestock Science* **155**, 186-96.

Riley P.A. & Borovansky J. (2011) Melanins and Melanosomes Biosynthesis, Biogenesis, Physiological, and Pathological Functions Preface. *Melanins and Melanosomes: Biosynthesis, Biogenesis, Physiological, and Pathological Functions*, Xv-Xvii.

Robinson J.T., Thorvaldsdottir H., Winckler W., Guttman M., Lander E.S., Getz G. & Mesirov J.P. (2011) Integrative genomics viewer. *Nature Biotechnology* **29**, 24-6.

Rolf M. (2015) Color Patterns in Crossbred Beef Cattle. Oklahoma State University, Oklahoma Cooperative Extension Service.

Rosengren Pielberg G., Golovko A., Sundstrom E., Curik I., Lennartsson J., Seltenhammer M.H., Druml T., Binns M., Fitzsimmons C., Lindgren G., Sandberg K., Baumung R., Vetterlein M., Stromberg S., Grabherr M., Wade C., Lindblad-Toh K., Ponten F., Heldin C.H., Solkner J. & Andersson L. (2008) A cis-acting regulatory mutation causes premature hair graying and susceptibility to melanoma in the horse. *Nat Genet* **40**, 1004-9.

Roulin A., Riols C., Dijkstra C. & Ducrest A.L. (2001) Female plumage spottiness signals parasite resistance in the barn owl (Tyto alba). *Behavioral Ecology* **12**, 103-10.

Santschi E.M., Purdy A.K., Valberg S.J., Vrotsos P.D., Kaese H. & Mickelson J.R. (1998) Endothelin receptor B polymorphism associated with lethal white foal syndrome in horses. *Mamm Genome* **9**, 306-9.

Sargolzaei M., Chesnais J.P. & Schenkel F.S. (2014) A new approach for efficient genotype imputation using information from relatives. *BMC Genomics* **15**, 478.

Scheet P. & Stephens M. (2006) A fast and flexible statistical model for large-scale population genotype data: applications to inferring missing genotypes and haplotypic phase. *American Journal of Human Genetics* **78**, 629-44.

Schmidt-Kuntzel A., Eizirik E., O'Brien S.J. & Menotti-Raymond M. (2005) Tyrosinase and tyrosinase related protein 1 alleles specify domestic cat coat color phenotypes of the albino and brown loci. *J Hered* **96**, 289-301.

Schmutz S.M. & Berryere T.G. (2007) Genes affecting coat colour and pattern in domestic dogs: a review. *Anim Genet* **38**, 539-49.

Schmutz S.M., Berryere T.G., Ciobanu D.C., Mileham A.J., Schmidtz B.H. & Fredholm M. (2004) A form of albinism in cattle is caused by a tyrosinase frameshift mutation. *Mamm Genome* **15**, 62-7.

Schmutz S.M., Berryere T.G. & Dreger D.L. (2009) MITF and White Spotting in Dogs: A Population Study. *Journal of Heredity* **100**, S66-S74.

Schmutz S.M. & Dreger D.L. (2013) Interaction of MC1R and PMEL alleles on solid coat colors in Highland cattle. *Anim Genet* **44**, 9-13.

Scholl F.A., Kamarashev J., Murmann O.V., Geertsen R., Dummer R. & Schafer B.W. (2001) PAX3 is expressed in human melanomas and contributes to tumor cell survival. *Cancer Research* **61**, 823-6.

Seitz J.J., Schmutz S.M., Thue T.D. & Buchanan F.C. (1999) A missense mutation in the bovine MGF gene is associated with the roan phenotype in Belgian Blue and Shorthorn cattle. *Mammalian Genome* **10**, 710-2.

Shin Y., Jung H.J., Jung M., Yoo S., Subramaniyam S., Markkandan K., Kang J.M., Rai R., Park J. & Kim J.J. (2016) Discovery of Gene Sources for Economic Traits in Hanwoo by Whole-genome Resequencing. *Asian-Australas J Anim Sci* **29**, 1353-62.

Siddiq A., Couch F.J., Chen G.K., Lindstrom S., Eccles D., Millikan R.C., Michailidou K., Stram D.O., Beckmann L., Rhie S.K., Ambrosone C.B., Aittomaki K., Amiano P.,

Apicella C., Australian Breast Cancer Tissue Bank I., Baglietto L., Bandera E.V., Beckmann M.W., Berg C.D., Bernstein L., Blomqvist C., Brauch H., Brinton L., Bui Q.M., Buring J.E., Buys S.S., Campa D., Carpenter J.E., Chasman D.I., Chang-Claude J., Chen C., Clavel-Chapelon F., Cox A., Cross S.S., Czene K., Deming S.L., Diasio R.B., Diver W.R., Dunning A.M., Durcan L., Ekici A.B., Fasching P.A., Familial Breast Cancer S., Feigelson H.S., Fejerman L., Figueroa J.D., Fletcher O., Flesch-Janys D., Gaudet M.M., Consortium G., Gerty S.M., Rodriguez-Gil J.L., Giles G.G., van Gils C.H., Godwin A.K., Graham N., Greco D., Hall P., Hankinson S.E., Hartmann A., Hein R., Heinz J., Hoover R.N., Hopper J.L., Hu J.J., Huntsman S., Ingles S.A., Irwanto A., Isaacs C., Jacobs K.B., John E.M., Justenhoven C., Kaaks R., Kolonel L.N., Coetzee G.A., Lathrop M., Le Marchand L., Lee A.M., Lee I.M., Lesnick T., Lichtner P., Liu J., Lund E., Makalic E., Martin N.G., McLean C.A., Meijers-Heijboer H., Meindl A., Miron P., Monroe K.R., Montgomery G.W., Muller-Myhsok B., Nickels S., Nyante S.J., Olswold C., Overvad K., Palli D., Park D.J., Palmer J.R., Pathak H., Peto J., Pharoah P., Rahman N., Rivadeneira F., Schmidt D.F., Schmutzler R.K., Slager S., Southey M.C., Stevens K.N., Sinn H.P., Press M.F., Ross E., Riboli E., Ridker P.M., Schumacher F.R., Severi G., Dos Santos Silva I., Stone J., Sund M., Tapper W.J., Thun M.J., Travis R.C., Turnbull C., Uitterlinden A.G., Waisfisz Q., Wang X., Wang Z., Weaver J., Schulz-Wendtland R., Wilkens L.R., Van Den Berg D., Zheng W., Ziegler R.G., Ziv E., Nevanlinna H., Easton D.F., Hunter D.J., Henderson B.E., Chanock S.J., Garcia-Closas M., Kraft P., Haiman C.A. & Vachon C.M. (2012) A meta-analysis of genome-wide association studies of breast cancer identifies two novel susceptibility loci at 6q14 and 20q11. *Human Molecular Genetics* **21**, 5373-84.

Silvers W.K. (1979) *The Coat Colors of Mice: A Model for Mammalian Gene Action and Interaction*. New York Heidelberg Berlin.

Simon J.D., Peles D., Wakamatsu K. & Ito S. (2009) Current challenges in understanding melanogenesis: bridging chemistry, biological control, morphology, and function. *Pigment Cell Melanoma Res* **22**, 563-79.

Sitaram A. & Marks M.S. (2012) Mechanisms of protein delivery to melanosomes in pigment cells. *Physiology (Bethesda)* **27**, 85-99.

Slominski A. & Paus R. (1993) Melanogenesis Is Coupled to Murine Anagen - toward New Concepts for the Role of Melanocytes and the Regulation of Melanogenesis in Hair-Growth. *Journal of Investigative Dermatology* **101**, S90-S7.

Slominski A., Wortsman J., Plonka P.M., Schallreuter K.U., Paus R. & Tobin D.J. (2005) Hair follicle pigmentation. *J Invest Dermatol* **124**, 13-21.

Steingrimsson E., Copeland N.G. & Jenkins N.A. (2004) Melanocytes and the microphthalmia transcription factor network. *Annual Review of Genetics* **38**, 365-411.

Steingrimsson E., Copeland N.G. & Jenkins N.A. (2005) Melanocyte stem cell maintenance and hair graying. *Cell* **121**, 9-12.

The UniProt Consortium (2017) UniProt: the universal protein knowledgebase. *Nucleic Acids Research* **45**, D158-D69.

Tobin D.J. & Paus R. (2001) Graying: gerontobiology of the hair follicle pigmentary unit. *Exp Gerontol* **36**, 29-54.

Van der Auwera G.A., Carneiro M.O., Hartl C., Poplin R., Del Angel G., Levy-Moonshine A., Jordan T., Shakir K., Roazen D., Thibault J., Banks E., Garimella K.V., Altshuler D., Gabriel S. & DePristo M.A. (2013) From FastQ data to high confidence variant calls: the

Genome Analysis Toolkit best practices pipeline. *Curr Protoc Bioinformatics* **43**, 11 0 1-33.

Vaz-Drago R., Custodio N. & Carmo-Fonseca M. (2017) Deep intronic mutations and human disease. *Human Genetics* **136**, 1093-111.

Videira I.F., Moura D.F. & Magina S. (2013) Mechanisms regulating melanogenesis. *Anais Brasileiros De Dermatologia* **88**, 76-83.

Walker W.P. & Gunn T.M. (2010a) Piecing together the pigment-type switching puzzle. *Pigment Cell Melanoma Res* **23**, 4-6.

Walker W.P. & Gunn T.M. (2010b) Shades of meaning: the pigment-type switching system as a tool for discovery. *Pigment Cell Melanoma Res* **23**, 485-95.

Wolf Horrell E.M., Boulanger M.C. & D'Orazio J.A. (2016) Melanocortin 1 Receptor: Structure, Function, and Regulation. *Front Genet* **7**, 95.

Womack T. (2015) Characterization of a Major Locus Affecting Coat Color Reddening in Cattle. In: *Animal Science*, p. 26. Texas A&M University.

Wong A.K., Ruhe A.L., Robertson K.R., Loew E.R., Williams D.C. & Neff M.W. (2013) A de novo mutation in KIT causes white spotting in a subpopulation of German Shepherd dogs. *Anim Genet* **44**, 305-10.

Wu Q. (2007) The serine protease corin in cardiovascular biology and disease. *Front Biosci* **12**, 4179-90.

Wu X.S., Martina J.A. & Hammer J.A., 3rd (2012) Melanoregulin is stably targeted to the melanosome membrane by palmitoylation. *Biochem Biophys Res Commun* **426**, 209-14.

Yamaguchi Y., Brenner M. & Hearing V.J. (2007) The regulation of skin pigmentation. *Journal of Biological Chemistry* **282**, 27557-61.

Yan S.Q., Hou J.N., Bai C.Y., Jiang Y., Zhang X.J., Ren H.L., Sun B.X., Zhao Z.H. & Sun J.H. (2014) A base substitution in the donor site of intron 12 of KIT gene is responsible for the dominant white coat colour of blue fox (Alopex lagopus). *Anim Genet* **45**, 293-6.

Yusnizar Y., Wilbe M., Herlino A.O., Sumantri C., Noor R.R., Boediono A., Andersson L. & Andersson G. (2015) Microphthalmia-associated transcription factor mutations are associated with white-spotted coat color in swamp buffalo. *Anim Genet* **46**, 676-82.

Zecca L., Tampellini D., Gerlach M., Riederer P., Fariello R.G. & Sulzer D. (2001) Substantia nigra neuromelanin: structure, synthesis, and molecular behaviour. *Mol Pathol* **54**, 414-8.

Zhou X. & Stephens M. (2012) Genome-wide efficient mixed-model analysis for association studies. *Nat Genet* **44**, 821-4.

Zimin A.V., Delcher A.L., Florea L., Kelley D.R., Schatz M.C., Puiu D., Hanrahan F., Pertea G., Van Tassell C.P., Sonstegard T.S., Marcais G., Roberts M., Subramanian P., Yorke J.A. & Salzberg S.L. (2009) A whole-genome assembly of the domestic cow, Bos taurus. *Genome Biology* **10**, R42.